DFT Study of the Electronic Structure of Neutral, Cationic and Anionic States of DNA –

Role of the phosphate backbone

CHAN Sze-ki

A thesis submitted in Partial Fulfilment
of the requirements for the Degree of
Master of Philosophy
in Chemistry

© The Chinese University of Hong Kong
December 2004

Master of Philosophy (2005)　　　　The Chinese University of Hong Kong
(Chemistry)

Title:　　　DFT study of Electronic Structure of Neutral, Cationic and Anionic States
　　　　　　of DNA – Role of the Phosphate Backbone

Author:　　Iris S. K. Chan

Supervisor:　Prof. Steve C. F. Au-Yeung

Abstract

This study examines the changes in the electronic structure of guanine, cytosine, adenine and thymine in their neutral, cationic and anionic state. All four nucleotides were studied using Density Functional Theory (DFT) at the B3LYP/6-311+g* level of theory and their optimized structure in the neutral form are compared to the relevant experimental data (3, 41). For each nucleotide, all structural components of a nucleotide, i.e. the base and the phosphate backbone, which includes the sugar and the phosphate groups, were included in the study.

The DFT result suggest that the adiabatic ionization potential (AIP) and adiabatic electron affinity (AEA) follow the trend in the decreasing order of T > A > C > G. Natural Population Analysis (NPA) and Molecular Orbital (HOMO and LUMO) Analysis reveal a similar observed trend for all four cationic nucleotides. It suggests that ??? is most likely required from the base.

Of the three basic structural components of a nucleotide, the results of this study show that the base is the most electron deficient when an electron is removed from the nucleotide. In the anionic state, the excess charges are distributed evenly between the base and the phosphate in guanine and cytosine, which renders both groups to become electron rich. In thymine and adenine, excess charges are localized on phosphate groups. These results confirm that the phosphate backbone does not play an important role in cationic molecules of DNA but it has a very important function in the anion form.

摘要

本論文研究了 G，C，A，T 在中性、陽離子及陰離子狀態下的電子結構。使用了密廣泛函之法下的 B3LYP/6-311+g*基組去研究核酸的結構，例如：碱基，磷酸骨架(包括糖和磷酸基)，四個優化後的中性核酸同實驗結果通行了比較 (3, 41)。從 AIP 和 AEA 的結果我們可以看到 T > A > C > G。NPA 和分子軌道 (HOMO 和 LUMO) 分析在陰離子狀態可以看到相類似結果，因此可知碱基在其中起了決定性作用。在陽離子狀態下，G 和 C 的磷酸基和碱基都有參予作用，但是在陰離子狀態下，磷酸骨架的作用不明顯。然而，在陽離子狀態下的 A 和 T，磷酸基有較強的作用，但是在陰離子狀態下，A 和 T 的磷酸骨架的作用不明顯。

ACKNOWLEDGEMENTS

I would like to express my sincere thanks to my supervisor, Prof. Steve C. F. Au-Yeung for his guidance, encouragement and supports throughout this study. Within these two years, I learnt a lot from him.

I wish to thanks Mr. Frank Ng and my groupmates. I also give my heartfelt thanks to my family and friends for their support and encouragement.

TABLE OF CONTENTS

List of Tables

Chapter 4

List of Figures

Chapter 1

Introduction

The basic background of Deoxyribonucleic acid (DNA) and the current status of the field are briefly reviewed. The first part is the background and structure of Deoxyribonucleic acid (DNA). The second part reviews the current understanding of charge distribution and transfer along DNA. The last part deals with the objective of this thesis.

1.1. Structure of Deoxyribonucleic acid (DNA)

1.1.1. Configuration and Conformation of Deoxyribonucleic Acid (DNA)

Deoxyribonucleic acid (DNA) is a hereditary material and a linear polymer composed of deoxyribonucleotide units. The nucleotide is not only the building block of the polynucleotides DNA but it also exhibits independent biological functions. The nucleotide consists of a nitrogenous base, a sugar and one or more phosphate group. The sugar is the deoxyribose. (1-4)

The nitrogen base is a derivative of purine or pyrimidine. The purines in DNA are guanine (G) and adenine (A); the pyrimidines are thymine (T) and cytosine (C). (Figure 1.1) The nucleoside is formed by attaching to the base through the C-1 of deoxyribose sugar, and for purine the attachment is through the N-9 atom in purine and for pyrimidine it is through the N-1 atom. The configuration of this N-glycosidic linkage is β.
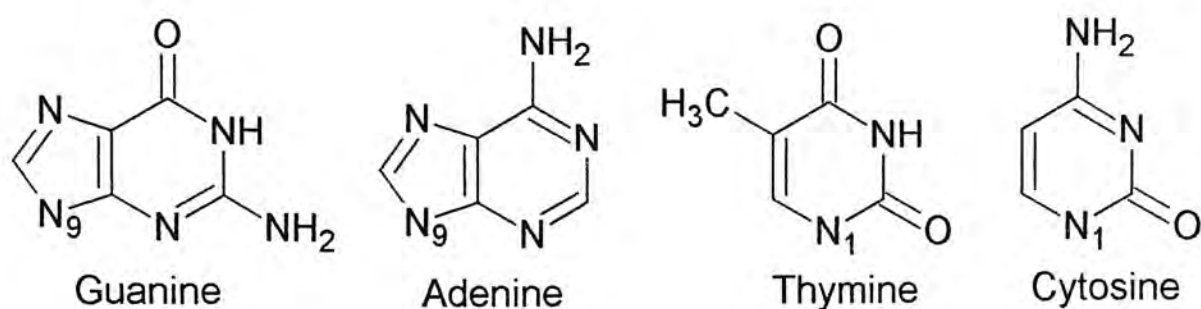
Figure 1.1   The chemical structure of bases: purine: guanine (G), adenine (A);
pyrimidine: thymine (T) and Cytosine (C) (1)

The base of DNA molecules carries genetic information, whereas their sugar and

phosphate groups perform a structural role. (1) The nucleotides are formed by adding

phosphate groups to nucleosides. In DNA, phosphate esters can be made at 3'- and 5'-

OH groups. Thus, the base sequence is written in the 5' – 3' direction. (Figure 1.2)
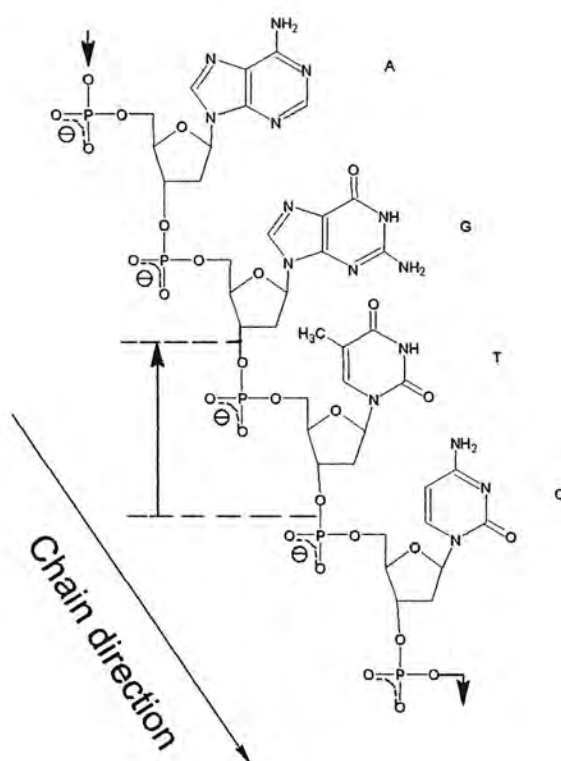
Figure 1.2   Fragment of deoxyribonucleic acid (DNA) with sequence adenine (A),
guanine (G), thymine (T) and cytosine (C) linked by 3',
5'-phosphodiester bonds. Chain direction is from 5', to 3'-end as
shown by arrow. (1)

1.1.2. Torsion Angle

The conformation of nucleosides and nucleotides depend on the torsion angles for rotation about each bond as defined by IUPAC convention. (2) There are seven torsion angles per nucleotide that must be specified to characterize the conformation (secondary structure) of a nucleic acid. (Figure 1.3)
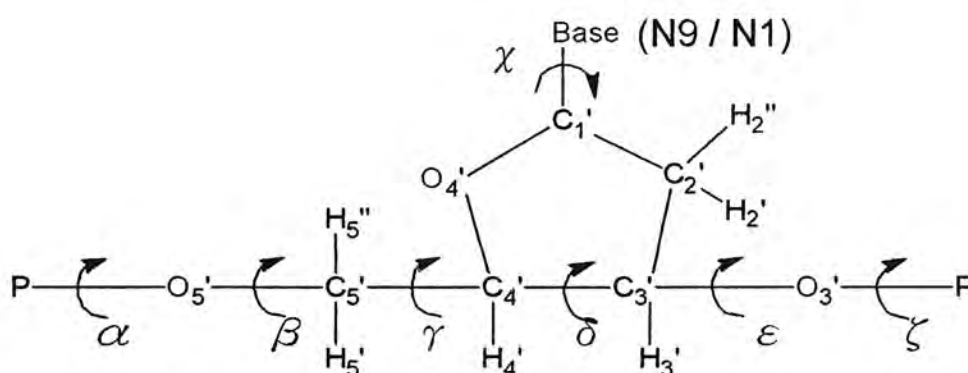
Figure 1.3   The seven torsion angles that specify the conformation of each nucleotide in a polynucleotide chain. The sugar-phosphate is characterized by six torsion angles (α, β, γ, δ, ε, ζ). The orientation of the base relative to sugar is specified by the glycosidic torsion angle, χ. (2)

In nucleotides, each base is attached to the 1' carbon of the sugar by a glycosidic bond to N1 in pyrimidines and to N9 in purines. The torsion angle about this bond is specified by the angle χ (Figure 1.3). The two ranges found for this angle are designated syn and anti. (2, 3, 4) The anti conformation is usually more stable. It is mostly found in mononucleotides and in right-handed double-stranded polynucleotides. In anti, the bulk of the heterocycles, the six-membered pyrimdine ring in purines and in pyrimidines, is pointing away from the sugar. The syn conformation requires some external stabilizing force. In the syn conformation the six-membered ring pf the purines or the carbonyl at C2 of the pyrimidines is over the sugar. This causes steric interference. The syn conformation can be favored by

3

attaching a bulky group at the 8 the position of purines or the 6 the position of pyrimidines.

Besides these seven torsion angles, five torsion angles, also called endocyclic sugar torsion angles, can be specified in a five-membered ring as shown in Fig. 1.4. The torsion angle C4'-O4'-C1'-C2' is v_0, and the v_1, v_2, v_3, v_4 continue clockwise around the ring.

Table 1.1

Definition of anti and syn conformational ranges. (2)

χ	$O_{4'}$—$C_{1'}$—N_9—C_4 (purine nucleotides)
	$O_{4'}$—$C_{1'}$—N_9—C_4 (pyrimidine nucleotides)
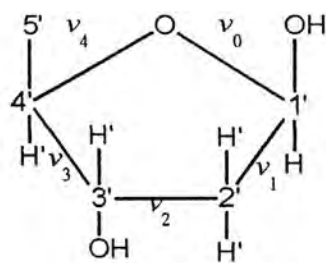
Figure 1.4   The structure and labeling scheme of a sugar ring (2)

A planar five-membered sugar ring (all torsion angles equal to zero) is sterically and energetically unfavorable. By displacement of one atom out of the plane, the strain is released and the energy is lowered to produce a stable conformation. If the five-membered ring is unsymmetrically constituted as in nucleotides, potential energy thresholds are created which limit the pesudotrataion and would lead to preferred puckering mode. Pucker modes can take the form of an envelope (E) with four atoms in a plane and the fifth atom is out or in a twist (T) form with two adjacent atoms displaced opposite sides of a plane through the other three atoms. Sugar puckering

4

modes are defined accordingly and are shown in Fig 1.5. It should be noted that because the transition between E and T forms is facile. In nucleotide, the pseudorotation phase angle P is calculated from the endocyclic sugar torsion angles according to the following equation and it leads to preferred puckering modes on the sugar (1)

$$\tan P = \frac{(v4 + v1) - (v3 + v0)}{2 \bullet v2(\sin 36^0 + \sin 72^0)}$$
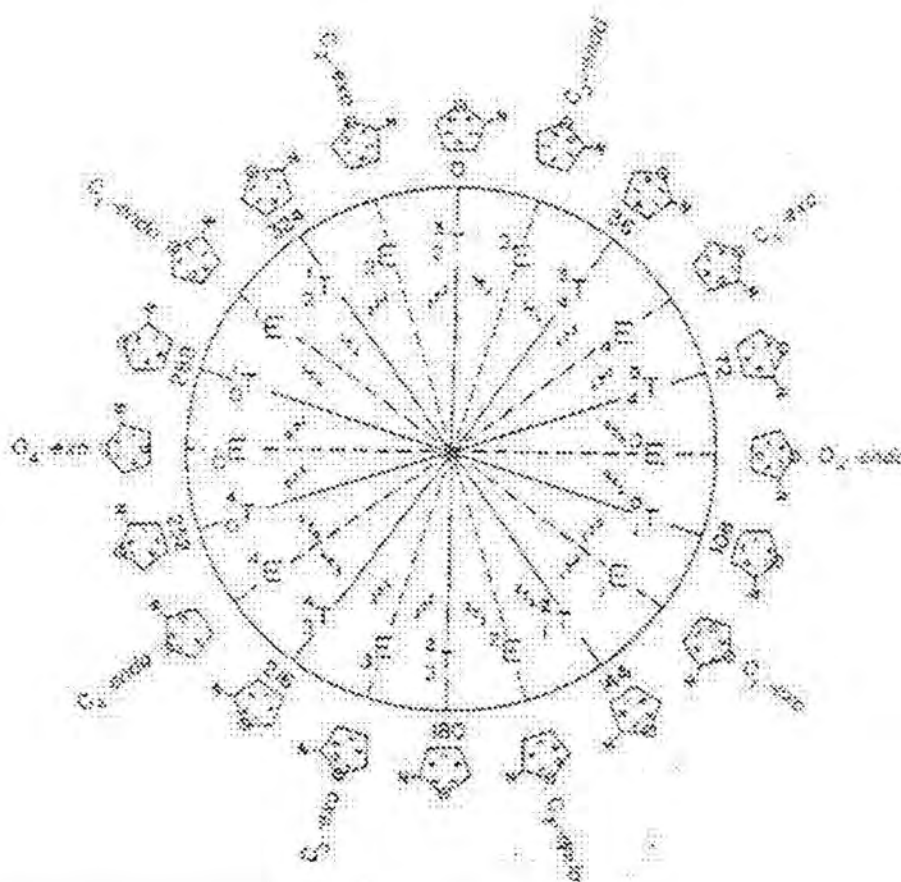
Figure 1.5   Pseudorotation cycle of the furanose ring in the nucleosides. Values of phase angles given in multiples of 36°. Envelope and twist T forms alternate every 18°. After rotation by 180° the mirror image of the starting position is found. On the periphery of the cycle, ribose with signs of endocyclic torsion angles are indicated. (+) Positive, (-) Negative, (0) angle at O°. (1)

5

1.1.3. Base Pairing

Standard Watson-Crick base pairs are formed by specific recognition between a purine and pyrimidine base, i.e. adenine paired with thymine and guanine paired with cytosine. These combinations lead to virtually identical base geometries as illustrated in Figure 1.6. A:T basepair is maintained and stabilized by two hydrogen bonds whereas G:C basepair has three hydrogen bonds. In general, G:C pairs are less readily deformed or broken within DNA than A:T pairs.

The G·C and A·T base pairs have the same distance between the C1' atoms of their sugars and can form a regular helix of any sequence. Each nucleic acid double helix has a major groove and a minor groove; the minor groove is the side of the base pair where the sugar is attached (2).
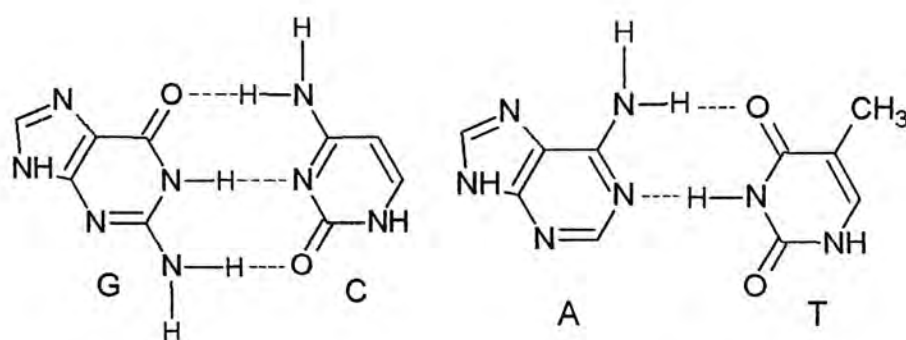
Figure 1.6 Waston-Crick base pairs found in the usual double-stranded DNA.

The minor groove is partly shielded by sugar-phosphate backbones; therefore many of interactions with nucleic acids are on the side of the major groove. The characteristic groups in the two grooves are shown in Table 1.2.

Table 1.2

Major and minor groove of four bases

	Major Groove	Minor Groove
G	C6 (carbonyl group), N7	N2 (amino), N3
C	N4 (amine)	C2 (carbonyl)
A	N6 (amino), N7	N3
T	C4 (carbonyl), C5 (methyl)	C2 (carbonyl)

1.2. DNA Damage

Radiation biologists discovered that radiolysis of water generates oxygen free radicals, which are responsible for many of consequences of irradiating living things. The characterization of radiation-induced oxidative DNA lesions and the connection between radiation have caused a surge of interest in DNA oxidants per second and raised the possibility of DNA damage from biological oxidants. Radiation, carcinogens, and metabolic waste products can damage DNA. It may cause mutations or carcinogenesis when lack of the repairmen. A study of electron transfer and radical-cation migration in DNA can provide valuable information for understanding DNA damage. A greater understanding of DNA-mediate electron transfer may have an additional clinical impact through the development of novel diagnostics tools. The centralism among biochemists, biologists, and toxicologists is: "How many oxidative DNA damages are there how does the radical get there, how and where is it removed, and what are the consequence?" Hence, we a brief summarize recent studies in this area. (5, 6)

Oxidative cleavage of DNA by ionization radiation, chemical oxidation, or photooxidation occurs more readily at guanine than at the other three common

nucleobases (7 - 9). This observation is consistent with the lower oxidation potential of guanine, as determined by electrochemical measurements on isolate nucleotides (Table 1.3). Table 3 shows the oxidation potential. The normally observed order of reactivity is GT or GC< GA < GG < GGG (10) since stacked Gs such as G doublet (GG) and triplet (GGG) possess much lower IPs (11 – 15) than that of isolated G. The GG's can serve as an effective hole trap (11). Selective cleavage at GG and GGG sites has been attributed to hole localization at these sites. (16 – 19)

Table 1.3

Nucleobase oxidation potential (form experimental result) (10)

Base	E_{ox} (V)
Thymine (T)	1.9
Cytosine (C)	1.9
Adenine (A)	1.69
Guanine(G)	1.24

In previous studies, two distinct types of photoinduced electron transfer processes have been identified (20 – 22): (1) A single-step electron transfer process between an excited molecule and ground-state molecule separated by a variable number of base pairs; (2) Charge transport process, in which a cation radical (hole) is generated at a specific site and can migrate over long distances in DNA to a trap site where strand cleavage may occur.

A hopping mechanism takes place in the long range charge transfer in DNA (23, 24). Thus, long-range charge transfer in DNA consists of a series of short-range tunneling processes. Whereas the positive charge is transported by oxidation of guanines base (G) during hole transfer in mixed DNA sequences, the negative charged should be conducted by reduction of thymine (T) and cytosine (C) (25). This conclusion is

8

derived from the redox potentials of the bases, which are different for guanine (G) and adenine (A) and similar for thymine (T) and cytosine (C). Since guanine (G) is the base of lowest oxidation potential in DNA, transfer of the positive charge occurs by tunneling between the guanines. The rate of these tunneling steps depends strongly on the distance between the neighboring G bases. The positive charge is transported through the DNA until it reaches a GGG unit, which is trapped irreversibly.

In double strands where the $(A:T)_n$ sequences between the guanines are rather long (n $\geqq$ 3) (26 - 31), charges hop between guanines with each hopping step depends strongly upon the guanine to guanine distances (32). In strand where the $(A:T)_n$ sequences between guanines are long (n $\geqq$ 4), the adenines also act as charge carriers. In DNA strands where the guanines are separated from each charge from a guanine radical cation $(G\bullet+)$ to an adjacent adenine becomes faster than the direct transfer of this charge to the distant guanine. In strands where the $(A:T)_n$ sequence between the guanines are rather long (n $\geqq$ 4), also the adenine act as charge carriers. (32) the subsequent migration of the positive charge between the adenines (A-hopping) is so rapid that the length of the $(A:T)_n$ sequence plays a minor role. Once A is oxidized, the charge migrates in fast hopping steps between adjoining adenines until it reaches a G, so that the overall charge-transfer rate decrease only slowly with a further elongation of the $(A:T)_n$ bridge. (25, 32)

In a previous study of M.D. Sevilla, he studied the ionization potential (IP) and the electron affinity (EA) of four different bases (guanine, cytosine, adenine, and thymine) using ab intio molecular calculations method. The IP and EA trends are the same obtained in the study as the reported and are T > C > A > G. (33, 34). However, the order of IPs in base pairs is C > T >> A > G. (33 – 36, 58).

9

In the study of DNA base pair, proton-transfer reaction was found in cation and anion radicals. (37 - 40) For both anion and cation radicals, it is the proton at the N1 of guanine (G) site, that transfer to cytosine (C). The proton-transfer showed in
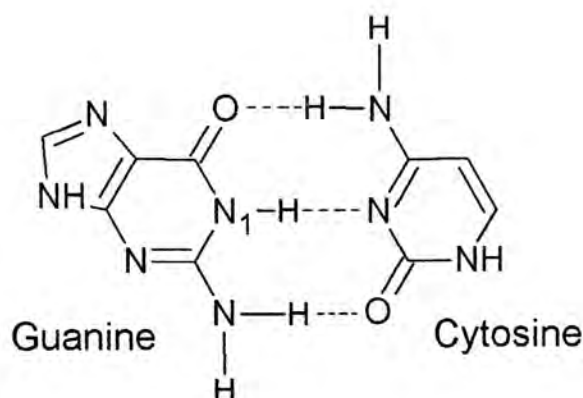
Figure 1.7   The proton transfer from guanine to cytosine

In the study carry out by of the Schaefer III (41 - 42), his work shows that excess charge resides on C in GC⁻ base pair. (41) The hydrogen bond between O6 of guanine (G) and H4 of Cytosine (C) is weakened resulting lengthening by the removal of electron density. Conversly, the hydrogen bonds between atom H1 of G and atom N3 of C (the middle H-bond) and between atom H2 of G and atom O2 of C are strengthened causing shortening bond length by increase of electron density. (Figure 1.8)
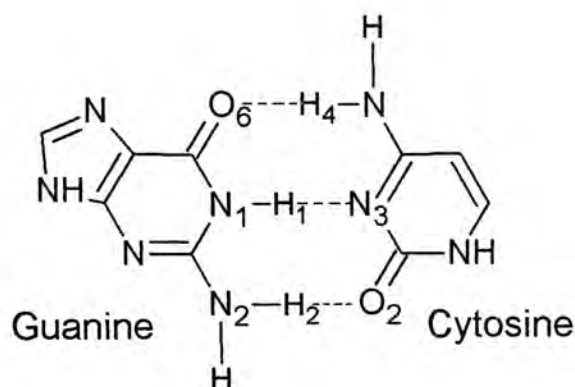
Figure 1.8   Three hydrogen bonds (H-bond) within base pair of guanine and cytosine

10

In the AT base pair, the anionic charge resides mostly on T which takes -0.94 of the excess electronic charge. The atoms O4, C4, and C6 show the greatest charge shifts. Such shifts in charge also account for the shortening of the H6-O4 and the lengthened of the N1-H3 hydrogen bonds as well as the lengthening of bonds in the T ring. (42)
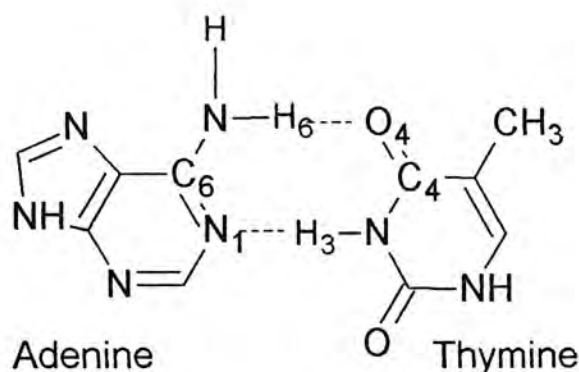
Figure 1.9   Two H-bonds within base pair of adenine and thymine

While the interaction of A and T provides some additional ability in bearing negative charges, the effect is less in GC. The study also showed that guanine (G) of double strand DNA is a better charge sink for positive charges and C is a better sink for negative charges, and the electron affinity of AT is less than that of GC even though the EA of isolated T is greater than that of isolated C.

1.3. The Objective of This Project

More understanding of the electronic structure and the properties of DNA is, expected to a good contribution in the investigation of diseases and in the development of pharmaceutical products.

The question of how charged species transferred over short or long distance in DNA remains unclear. A concerted worldwide research effort is underway to explain the large variations in observed electron transfer rates (microsecond to picosecond) and to develop well-defined chemical systems for further study. In earlier studies, the focus is on the base (guanine, cytosine, adenine, and thymine) of base. Majority of these projects studied electron-, proton-transfer within the basepair and the charge distribution in the DNA-base (guanine, cytosine, adenine, and thymine) without considering the effect of backbone (phosphate group and sugar). Since each function moiety has a role in the stabilizing the structure and/or the electronic charges, a systematic study of intact nucleotides including the phosphate groups and sugar is required because of together with the base, they form a complete basic unit. The objective of this project is designed o study:

1. the electronic structures (bond lengths, torsion angles and the puckering modes of sugar ring) of four nucleotides (guanine, cytosine, adenine, and thymine) at different states (neutral, cationic and anionic state).

2. the ionization potential and an electron affinity of all four nucleotides

3. the charge distribution and molecular orbitals (highest occupied molecular orbital, HOMO and lowest occupied molecular orbital, LUMO) of four nucleotides at different states

4. the effect of the components (base, sugar, phosphate groups) of DNA in different states

Chapter 2

Theory and Computational Details

This chapter is divided into five parts. In the first section, the basic theory of computational method and a brief summary discussing the Density Functional Theory (DFT) and basis set is given. Next, the definition of different types of ionization potential (IP) electron affinity (EA) will be reinsured. Thirdly, the Natural Bond Orbital (NBO) method is discussed the following by serving the molecular orbital method both features on the highest occupied molecular orbital (HOMO) and the lowest unoccupied molecular orbital (LUMO). The last part gives the details of the computational method used in this project.

2.1. Computation Theory

2.1.1. Density Functional Theory (DFT)

Ab initio (non-empirical) quantum chemical methods", based on the solution of time-independent Schrödinger equation, which are free of any empirical procedures/parameterization. This is the key point in understanding the important area of *ab initio* methods, because all other methods (semi-empirical methods, classical empirical force fileds) are based on parameterization. (43, 44)

In Hartree-Fock (HF) theory, the energy of a mutli-electron system is given by:

$$E^{HF} = E^{nuclear} + E^{core} + E^{coulomb} + E^{exchange}$$

where

$E^{nuclear}$ is the nuclear repulsion energy,

E^{core} is othe ne-electron (kinetic plus potential) energy,

$E^{coulomb}$ is the classical coulomb repulsion of the electrons,

$E^{exchange}$ is the exchange energy resulting from the quantum (fermion) nature of

electrons

In Density Functional Theory, the energy includes the nuclear energy, core energy,

coulomb energy and, the exchange-correlation functional, which includes terms

accounting for both exchange energy, $E^x(P)$, and the electron correlation which is

omitted in Hatree-Fock theory, $E^c(P)$:

$$E^{DFT} = E^{nuclear} + E^{core} + E^{coulomb} + E^{exchange} + E^x(P) + E^c(P)$$

$E^x(P)$, and $E^c(P)$ are functions of the electron density, P.

2.1.2. Closed-shell and Open-shell Determinantal Wavefunctions

Closed-shell single-determinant/Spin-restricted (RHF) (44) wavefunctions represent

the most commonly used form of HF theory and are appropriate for the description of

the ground states of most molecules with an even number of electrons (n). The

alternative open-shell procedure is the spin-unrestricted (UHF) method, in which the

orbitals associated with α and β electrons are treated completely independently. The

advantages of this method are: (a) that it generally gives a lower energy than the

corresponding RHF treatment, (b) that it is capable of providing a qualitatively correct

description of bond dissociation, and (c) that it is generally computationally more

efficient than the corresponding RHF procedure.

2.1.3. Calculation Method

Ab initio techniques are mainly applied to study nucleic acid bases and their complexes. Hartree Fock (HF) theory approximates the true multi-electron wavefunction. (44) However, HF method ignores correlation of electronic motions by assuming that electrons can move independently. The neglect of correlation energy leads to serious error. Density functional theory (DFT) belonging to family of *ab initio* methods is a method with inclusion of electron correlation. The DFT calculations provide reasonable values of amino group pyramidalization for nucleic acid bases and related compounds, very good dipole moments, charge distributions and vibrational frequencies. The density functional theory with the Becke three-parameter exchange functional B3-LYP s relatively efficient in evaluation of the molecular structure and particularly, vibrational frequencies and IR intensities of isolated base.

2.1.4. Basis Set Details

A basis set is the mathematical description of the orbitals within a system used to perform the theoretical calculation. (*) Larger basis sets more accurately approximate the orbitals by imposing fewer restrictions on the locations of the electrons in space. In a true quantum mechanical picture, electrons have a finite probability of existing anywhere in space; this limit corresponds to infinite basis set expansion.

Minimal basis sets use fixed-size atomic-type orbitals. The STO-3G basis set is a minimal basis set. To form a large basis set, the first method is to increase the number

of functions per atom, for example, using Split valance basis sets (such as 6-311G.). (43, 44)

Split valance basis sets allow orbitals to change size, but not to change shape. Polarized basis set remove this limitation by adding orbitals with angular momentum beyond what is required for the ground state to the description of each atom. For example, the notation 6-311G** means that the 6-311G basis set is used, and two shells of d-functions and one shell of f-functions are added to all non-hydrogen atoms, and two shells of p- and one shell of d-functions are added to all hydrogens.

Diffuse functions are large-size versions of s- and p- type functions. They allow orbitals to occupy a larger region of space. Basis sets with diffuse functions are important for systems where electrons are relatively far from the nucleus, for examples: molecule with lone pairs, anions and other systems with significant negative charge systems in their excited states, systems with low ionization potentials and so on. The 6-311+G** for first-row elements are constructed from the underlying 6-311G** representations by the addition of a single set of diffuse gaussian s- and p-type functions. (43, 44)

2.2. Ionization Potential and Electron Affinity

The adiabatic ionization potentials (AIP) were calculated by computing the difference in energy between optimized neutral nucleotides and corresponding optimized cation radical. For the vertical ionization potentials (VIP), (33, 40) the optimized geometries of the neutral nucleotides were also used to calculate the energies of the

corresponding cation radical. The adiabatic electron affinities (AEA) (40) were calculated by computing the difference in energy between optimized neutral nucleotides and corresponding optimized anion radical. For the vertical electron affinity (VEA), the optimized geometries of the neutral nucleotides were also used to calculate the energies of the corresponding anion radical. The difference between the adiabatic and vertical ionization potential/electron affinity yields reorganization energy. (40)

The physical meaning of AIP is the energy required when an electron is lost from the molecule without conformation changes. VIP is the energy required when an electron is lost from the system with a change in conformation. The reorganization energy is the conformation change after removing an electron from the molecule. (40)

The physical meaning of AEA is the energy required when an electron is added to the molecule without conformation changes. VEA is energy required when an electron is added to the system with a change in the conformation. The reorganization energy is the conformation change after addition of an electron to the molecule.

2.3. Natural Bond Orbital (NBO)

The NBO program performs the analysis of a multi-electron molecular wavefunction in terms of localized electron-pair bonding units. NBO analysis is based on a method for optimally transforming a given wavefunction into localized form, corresponding to the one-center ("lone pair") and two-center ("bond") elements of the chemist's Lewis structure picture. (45) NBO analysis is used to analyze the orbital interactions

It shows that the structure of T is the most flexible when compared with other nucleotides and that G is the least flexible. This observation agrees with experimental findings (34) that thymine can release the most energy to stabilize its structure.

3.2.2. Bond length

In guanine, after an electron is removed, the greatest charge shifts takes place in the base (Table 3.18) and the corresponding bond lengths changes is shown in Fig 3.9. Due to the charge-density rearrangement, the bond lengths in the base strengthen or shorten accordingly. For example, the bond lengths of C2-N3 ($\Delta = 0.5$ Å), C4-C5 ($\Delta = 0.4$ Å), C5-C6 ($\Delta = 0.06$ Å), N7-C8 ($\Delta = 0.04$ Å) and N9-C1' (sugar ring) ($\Delta = 0.06$ Å) increase whereas the bond lengths of C2-N2 ($\Delta = 0.04$ Å), N3-C4 ($\Delta = 0.04$ Å), C5-N7 ($\Delta = 0.04$ Å) and C8-C9 ($\Delta = 0.03$ Å) decrease.

Charge delocalization is expected in the base because it is composed of either 5- and/or 6-membered ring molecules. From the above results, bond lengths increase and decrease alternatively within the base, which consists of single and double bonds. The same results are observed in other nucleotides in which the bond lengths of DNA-base rearranged due to the relocalization of charges in the system. Base becomes more flexible because charges mainly declocalize in cation molecules. Therefore, adjustment of bond lengths is possible because tangible damage to the integrity of the structure is minimized upon removal of an electron. The discussion in rearrangement of charge density is delayed to sections 3.2.6 and 3.2.7.

Note that for the glycosidic bond N9/N1-C1', which connects the sugar and the base, increases but no change is observed in its bond length when an electron is removed.

of DNA nucleotides. It constitutes the basis of the natural population analysis (NPA). While atomic charge cannot be determined experimentally, the polarity of the molecule can be deduced from the direction of its electric dipole moment. Whereas the constituent nuclear charges are clearly atom-centered, the electron charge distribution is spread out over the entire molecule.

2.4. Molecular Orbital

Orbital interaction theory has its roots in molecular orbital (MO) theory. Molecular orbital theory in one form or another plays a central role in the understanding of all aspects of chemical phenomena. The electrons cannot be represented as point charges, as can be done with the nuclei. Instead, a mathematical function in three dimensions is assigned to each electron. This is its wave function. The wave function of a single electron is called an orbital. Whether it is an atomic orbital (AO) or a molecular orbital (MO) depends on whether one or more nuclei are present. (46, 47)

In the application of molecular orbital theory to molecules, the following assumptions have been made:

1. The consequence of inner core electrons will be disregarded.
2. Only the valence electrons which are usually the $p\pi$ electrons will be treated.
3. The linear combination of atomic orbitals (LCAO) approximation will be used to obtain the approximation will be used to obtain the appropriate molecular orbitals.
4. Electrons may be assigned to definite orbitals.

18

5. An electron in a particular orbital may be assigned a definite energy.

6. Only two nonidentical electrons may occupy a given orbitals.

7. The forces involved in chemical bonding are electrostatic in nature.

It is assumed that each orbitals (energy level) can only be populated by a maximum Two orbitals will have special significance for orbital interaction theory; the highest occupied molecular orbital (HOMO) because it represents the distribution and energy of the least tightly held electrons in the molecule and the lowest unoccupied molecular orbital (LUMO) because it describes the easiest route to the addition of more electrons to the system. In fact, the energy of the HOMO is a good approximation to the lowest ionization potential of the molecule but the energy of the LUMO generally is a poor approximation to the molecule's electron affinity. To probe the basicity or nucleophilicity, the interaction of a proton (empty s orbital) with the HOMO is sufficient. For checking acidity in the Lewis sense, the interaction of the LUMO with the HOMO is appropriate.

2.5. Computational Details in This Project

2.5.2. Calculation Method

Optimized geometries and natural charges were determined for the four DNA nucleotides. DFT theory using B3LYP density functional with a 6-311+G** basis set (48-51) was used. The structures of four nucleotides (guanine, cytosine, adenine, and thymine) in neutral, cationic, and anionic states have been studied. And frequency calculations of optimized structures have been studied. Natural population atomic (NPA) charges were determined at the B3LYP/6-311+G** level using the natural

bond order (NBO) analysis. All computations were performed for the gas phase
structures, without considering solvent effects.

2.5.3. *Studied Model*

In previous studied, the focuses have been on the change in the base (guanine,
cytosine, adenine, thymine), the effect of the backbone of DNA (phosphate group +
sugar) has not been considered. However, the system should be examined as a whole
since the backbone may have its special function in stabilizing the structure of DNA.
Base on the rationale, the studied models have included the backbone of DNA and
base and are shown below.
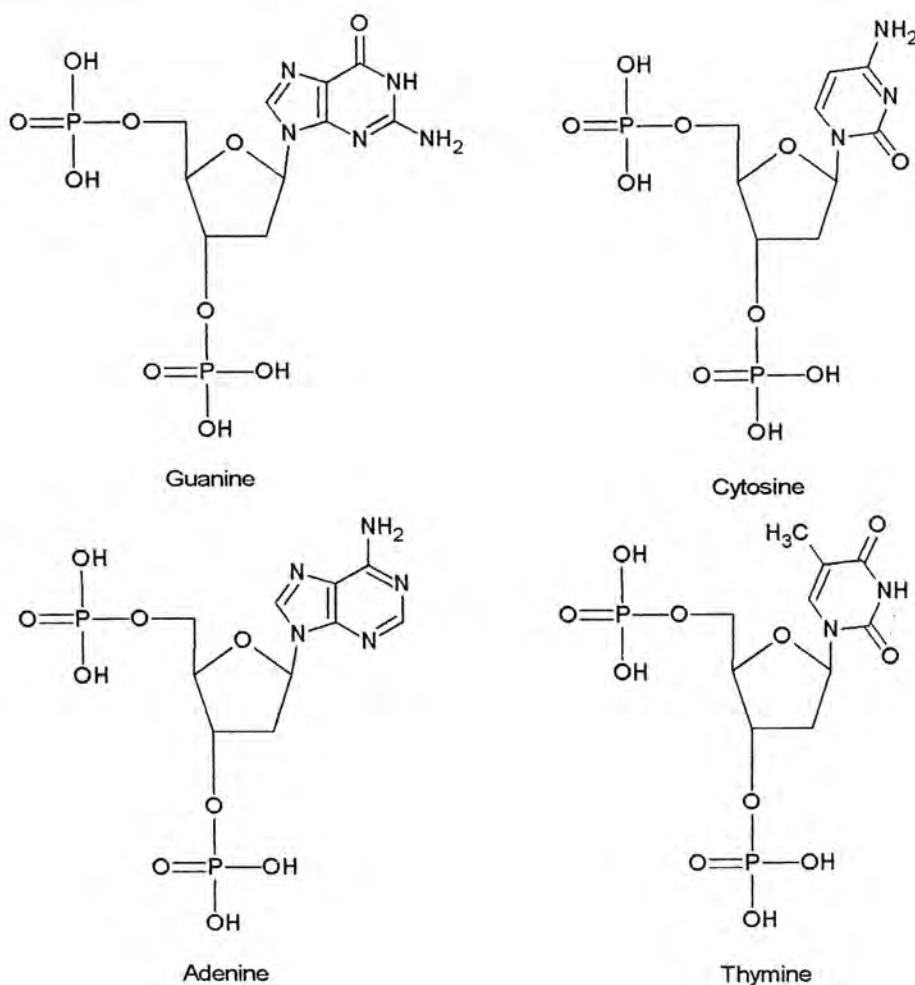
Figure 2.1   Studied model in this project

Chapter 3

Results and Discussions

This chapter presents a full discussion of the results obtained in this study. The discussion is structured according to the charge state of the nucleotides; namely calculation results of neutral, cationic and anionic states of guanine, cytosine, adenine and thymine.

3.1. The Neutral State

In the first two sections (3.1.1 and 3.1.2), results of bond lengths and torsion angles of all nucleotides optimized using B3LYP/6-311+G** are compared with the relevant experimental data. In the section(s) that follow, the sugar puckering modes in each nucleotide is also analyzed to determine its role as a charge sink upon oxidation or reduction. The charge distribution and molecular orbital of all nucleotides are examined in the last two parts with the objective of understanding the relationship of each component with their electronic structure.

3.1.1. Bond Length

All molecules are optimized at the B3LYP/6-311+G** level of theory. Bond lengths of all neutral nucleotides are summarized in Tables 3.1 -3.4. The atoms labeling scheme of models studied are shown in Figure 3.1.
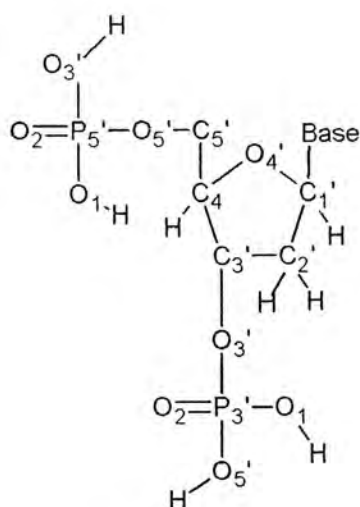
Figure 3.1   The atoms labeling scheme in nucleotide

The results show that the optimized geometry of the four neutral nucleotides are in good agreement with reported experimental data and relatively small deviations observed in bond distance and bond angle. Therefore, it is concluded that this calculation method is suitable for DNA models studied in this work.

Table 3.1

Calculated & experimental bond lengths of sugar ring of nucleotide

Sugar	Expt. Data *	Nucleotide			
		G	C	A	T
C4' – O4'	1.42	1.430	1.425	1.423	1.428
O4' – C1'	1.43	1.428	1.432	1.427	1.436
C1' – C2'	1.53	1.533	1.537	1.541	1.534
C2' – C3'	1.52	1.524	1.527	1.532	1.528
C3' – C4	1.54	1.538	1.542	1.551	1.542
C4' – H		1.091	1.090	1.092	1.090
C3' – H		1.082	1.080	1.081	1.080
C2' – H'		1.091	1.092	1.088	1.089
C2' – H"		1.088	1.088	1.092	1.088
C1' – H		1.092	1.087	1.090	1.092
C1' – N1/N9		1.451	1.454	1.448	1.452

* Ref. 52

Table 3.2

Calculated and experimental bond length of backbone results of neutral nucleotides

Backbone	Expt. Data *	Nucleotide			
		G	C	A	T
Attached P5'					
O3'-H		0.967	0.964	0.968	0.960
P5'-O3'	1.600	1.602	1.613	1.603	1.611
P5'-O2	1.480	1.478	1.476	1.482	1.478
P5'-O5'	1.600	1.602	1.598	1.599	1.596
P5'-O1	1.480	1.628	1.605	1.622	1.608
O1-H		0.961	0.962	0.960	0.962
O5'-C5'	1.440	1.452	1.450	1.452	1.448
C5'-H'		1.093	1.097	1.092	1.094
C5'-H"		1.095	1.091	1.092	1.096
C5'-C4'	1.516	1.522	1.518	1.517	1.519
Attached P3'					
O5'-H		0.961	0.964	0.968	0.966
O5'-P3'	1.600	1.603	1.622	1.625	1.608
P3'-O2	1.480	1.478	1.477	1.467	1.475
P3'-O3'	1.600		1.598	1.621	1.616
P3'-O1	1.480	1.614	1.618	1.588	1.604
O1-H		0.968	0.967	0.985	0.968
O3-C3'			1.458		1.457
The bond distance between two phosphate groups					
P5'-P3'		6.273	6.882	4.784	6.693
O3' (attached P5') – P3'		7.398	7.916	5.882	7.904
P5' – O5' (attached P3')		7.532	7.398	4.758	7.802
P5' - O2 (attached P3')		6.836	8.092	6.178	6.674
P5' – O1 (attached P3')		5.528	6.280	3.756	8.152
O1 (attached P5') – P3'		6.647	6.682	5.876	7.033
O2 (attached P5') – P3'		6.553	7.620	3.778	7.641

* Ref. 52
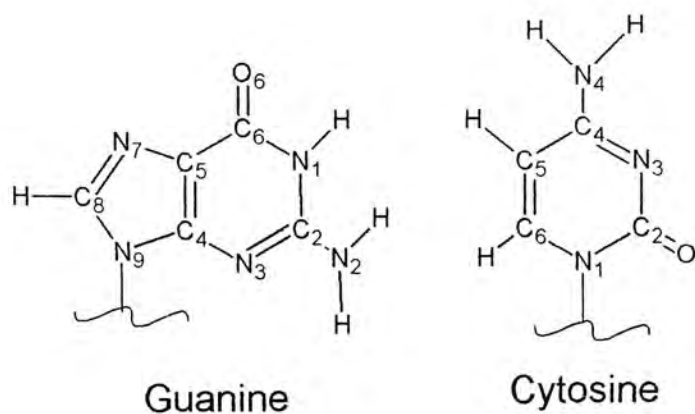
Figure 3.2   The structures of guanine and cytosine

Table 3.3

Calculated and experimental bond length data of neutral guanine and cytosine

G	Expt.	Calc.	C	Expt.	Calc.
N9 – C8	1.378	1.380	N1 – C6	1.360	1.358
C8 – N7	1.311	1.307	C6 – C5	1.357	1.356
N7 – C5	1.394	1.379	C5 – C4	1.433	1.438
C5 – C6	1.419	1.398	C4 – N4	1.324	1.360
C6 – O6	1.228	1.218	C4 – N3	1.339	1.318
C6 – N1	1.402	1.440	N3 – C2	1.358	1.368
N1 – C2	1.381	1.369	C2 – O2	1.237	1.224
C2 – N2	1.335	1.373	N1 – C2	1.392	1.438
C2 – N3	1.331	1.308			1.082
C4 – N3	1.359	1.352			1.084
C4 – N9	1.378	1.371			1.009
C4 – C5	1.375	1.390			1.012
C8 – H		1.072			
N1 – H		1.018			
N2 – H'		1.012			
N2 – H"		1.009			

• Ref. 52

24
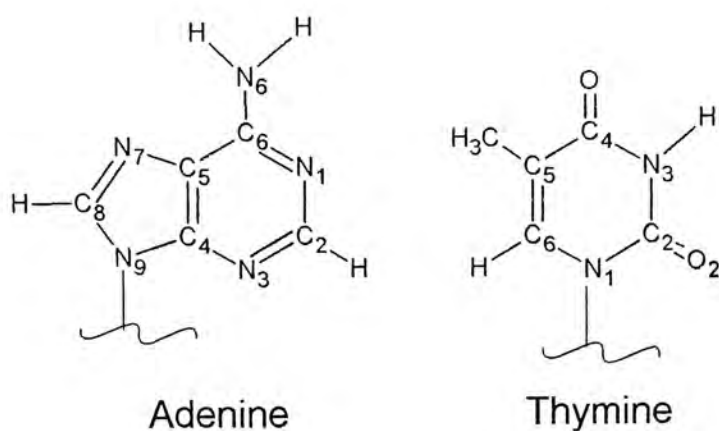
Figure 3.3   The structure of adenine and thymine

Table 3.4

Calculated and experimental bond length data of neutral adenine and thymine

A	Expt.	Calc.	T	Expt.	Calc.
N9 – C8	1.366	1.376	N1 – C6	1.370	1.382
C8 – N7	1.297	1.305	C6 – C5	1.343	1.342
N7 –C5	1.388	1.385	C5 – C4	1.444	1.463
C5 – C6	1.404	1.409	C4 – N3	1.380	1.396
C6 – N1	1.346	1.342	N3 – C2	1.381	1.384
N1 – C2	1.332	1.339	C2 – N1	1.374	1.388
C2 – N3	1.315	1.331	C6 – H		1.081
N3 – C4	1.349	1.338	C5 – C (methyl group)	1.500	1.496
C4 – N9	1.370	1.375	C (methyl group) – H1		1.090
C4 – C5	1.365	1.387	C (methyl group) – H2		1.089
C6 – N6	1.341	1.349	C (methyl group) – H3		1.088
C8 – H		1.068	C4 – O4	1.233	1.218
N6 – H1		1.003	N3 – H		1.012
N6 – H2		1.008	C2 – O2	1.219	1.220
C2 – H		1.078			

* Ref. 52

3.1.2. Torsion Angle of DNA Backbone

In the backbone of a nucleotide, there are seven torsion angles and Figure 1.3 provides a schematic definition. The backbone plays an important role in defining conformation properties of double-helical DNA. For example, the observed conformation of a dinucleotide basepair step is determined by a preferred stacking interaction and a preferred backbone conformation. (42, 54) Two important mechanisms exert control over the base stacking geometry in the backbone: (i) the backbone has finite length, therefore the conformational space accessible by the different bases are restricted; (ii) the backbone couples with the conformation properties of neighboring basepair steps within a sequence (43 – 45).

The calculation results of all four nucleotides are compared with single crystal x-ray structures data of oligodeoxynucleotides collected from the literature, which are presented in Table 3.5.

Table 3.5

Calculated DNA backbone torsion angles for all neutral nucleotides*

		Expt. Data **	G	C	A	T
Torsion Angle	α	270-330	289	314	286	313
	β	130-220	170	183	236	167
	γ	20-80	50	56	53	56
	δ	70-180	106	135	103	138
	ε	160-270	209	196	249	202
	ζ	230-300	180	294	179	267
		150-210				
	χ	200-300	289	227	237	242

*the statistical ranges of the torsion angles determined from DNA crystal structures

**Ref 52

The seven torsion angles span large ranges, indicating that the DNA backbone has large degrees of freedom. The experimental data range is determined from a statistical analysis of data extracted from different B-form DNA sequences in the literature. The results presented in Table (3.5 8?) show that almost all torsion angles fall well within established statistical ranges. Therefore, both bond angle and torsion angle results are in reasonable agreement with available experimental data. It reaffirms that the calculation method employed is suitable for the DNA models studied in this thesis.

Note also that the glycosylic torsion angles of all four nucleotides are in the anti-form, which is between $200° - 300°$ in B-form DNA and that the energy of the syn-conformation is higher than that of the anti-conformation (53). Only one torsion angle (β) in adenine is found to span a range outside the statistically determined data range. The range of β is $130° - 220°$, but the calculation result of β in adenine is $236°$ (52).

3.1.3. Sugar Ring Puckering Modes

The planar furanose ring is energetically unfavorable because all torsion angles are at $0°$ and the substituents attached to carbon atoms are fully eclipsed in this arrangement. However, puckering through its different conformations according to its torsion angles can minimize its energy. The pseudo-rotation phase angle, P, calculated from all five-torsion angles, is a useful probe to study the puckering modes. The results of sugar puckering modes of all four neutral nucleotides are summarized in Table 3.6.

Table 3.6

Conformation of sugar for G, C, A, T

(pseudo-rotation phase angle and puckering mode)

	G	C	A	T
Pseudo-rotation phase angle, P	327	146	100	180
Puckering Mode	$^{1}_{2}T$	$^{2}_{1}T$	$\%\,^{0}E/^{0}_{1}T$	$^{2}_{3}T$

The puckering modes of guanine and cytosine are $^{2}_{1}T$ and $^{1}_{2}T$ respectively, whereas

the pseudo-rotation phase angles (P) of guanine is $327°$ and that of cytosine is $146°$. In

other words, the conformation of guanine and that of cytosine are nearly $C_{2'}$-exo and

$C_{2'}$- endo respectively and are amongst the lowest energy conformations available in

the sugar (Fig 3.5). According to the pseudo-rotation cycle of the furanose ring (see

Fig 3.4), guanine's puckering mode is located symmetrically opposite that of

cytosine's puckering mode and that both $C_{2'}$-exo and $C_{2'}$- endo puckering modes are

stable conformations. In $C_{2'}$-exo or $C_{2'}$- endo, the furanose ring adapts conformations

with the C –O torsion angle v_0 nearly eclipsed (around $0°$) whereas C – C torsion

angles v_1, v_2, v_3 are maximally staged. Therefore in addition to the stability achieved

through the formation of the three H-bonds for guanine and cytosine, additional

stability is achieved through mutual compensation by providing a pathway for the

complementary base to release its energy and strengthen its linkage.

The pseudo-rotation phase angle (P) of adenine is $100°$ and its puckering mode is

between ^{0}E and $^{0}_{1}T$ and the conformation is nearly $O_{4'}$-endo. For thymine, the

pseudo-rotation phase angle is $180°$ with a puckering mode at $^{2}_{3}T$ whereas its

conformation is near to $C_{2'}$-endo. When compared against the other three nucleotides,

the sugar of adenine has the highest energy (Fig. 3.5) and its conformation can adapt both the twist and the boat forms. Therefore, this structure is less stable. In Standard Watson-Crick base-pairing scheme, adenine pairs up with thymine forming H-bonds. Although thymine is the complementary base of adenine, there is no symmetrical disposition found for the puckering modes of adenine and thymine (Fig 3.6). It implies that the reactivity of the AT basepair is higher than that of the GC basepair.
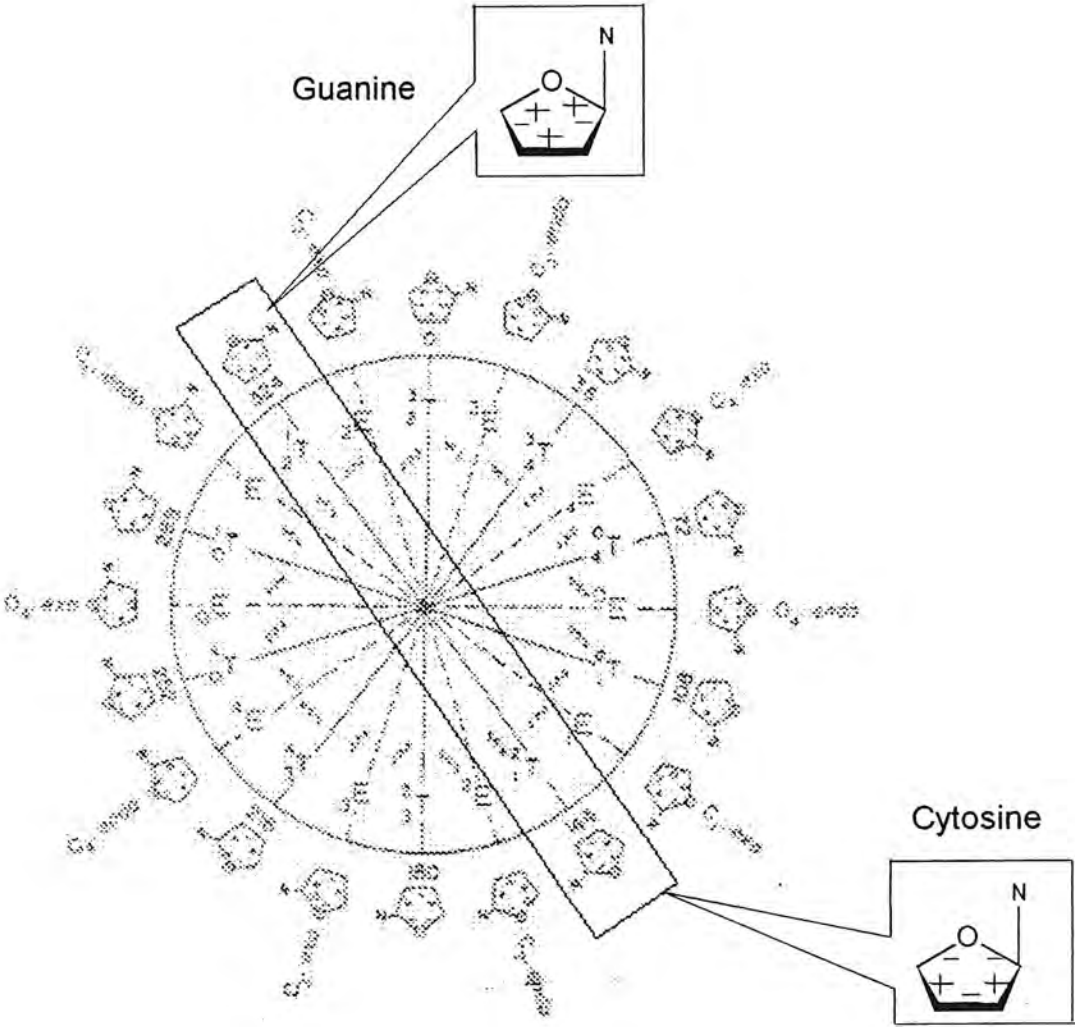
Fig 3.4   The puckering mode of guanine and cytosine (Adapted from Ref. 3.??)
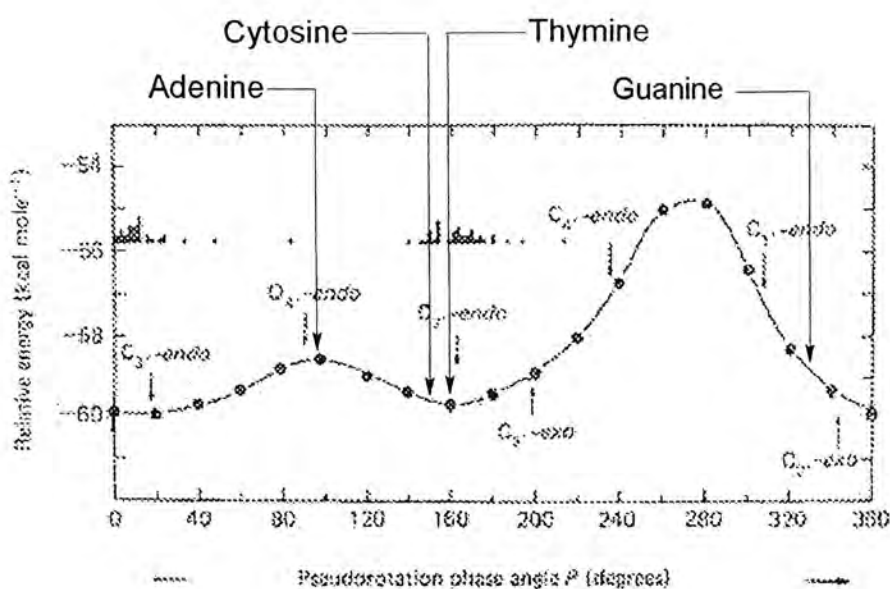
Fig 3.5   Variation

of total energy with pseudo-rotation phase angle P. Solid line calculated for all

five-endocyclic torsion angles v_n constricted to the pseudo-rotation path. Dot

histograms give phase angles P from nucleoside crystal structures. (Adapted from
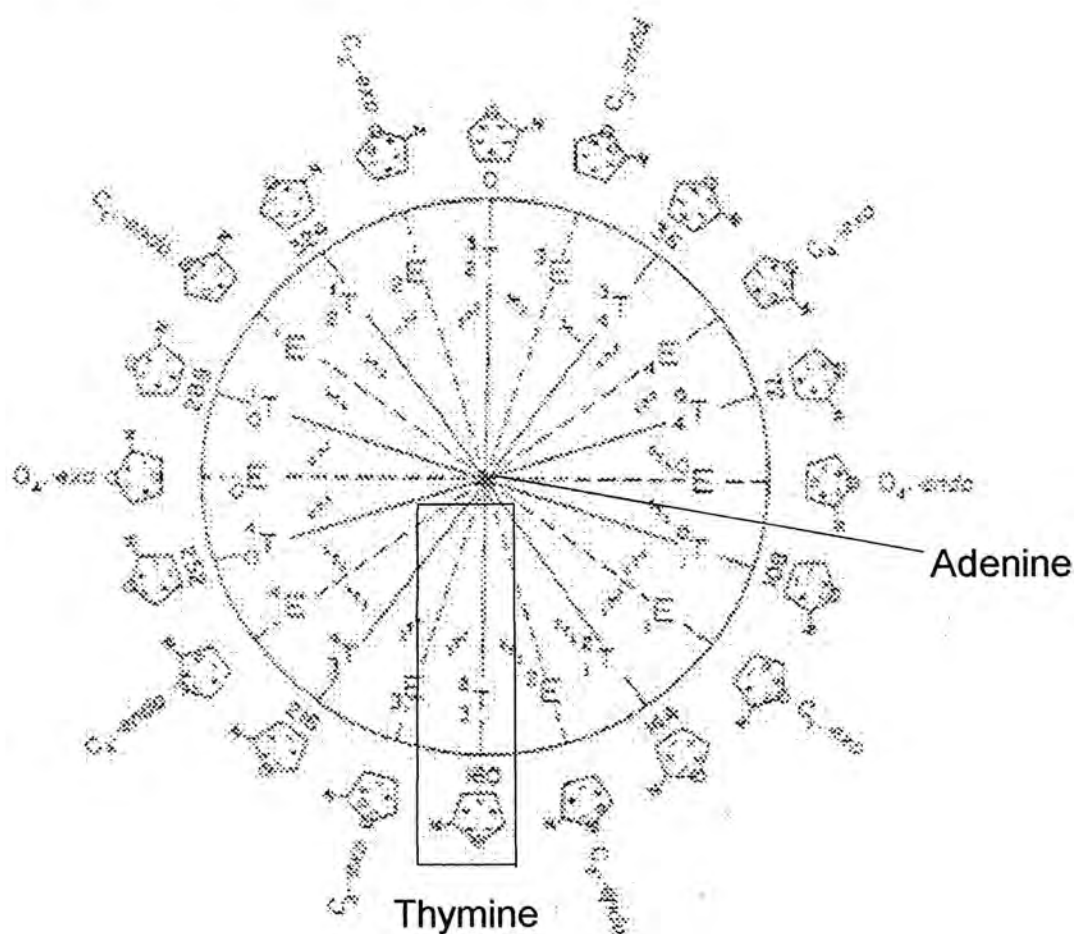
Principles of Nucleic Acid Structure (Ref. 1)

Fig 3.6 Puckering modes of adenine and thymine

3.1.4. Natural Population Analysis (NPA)
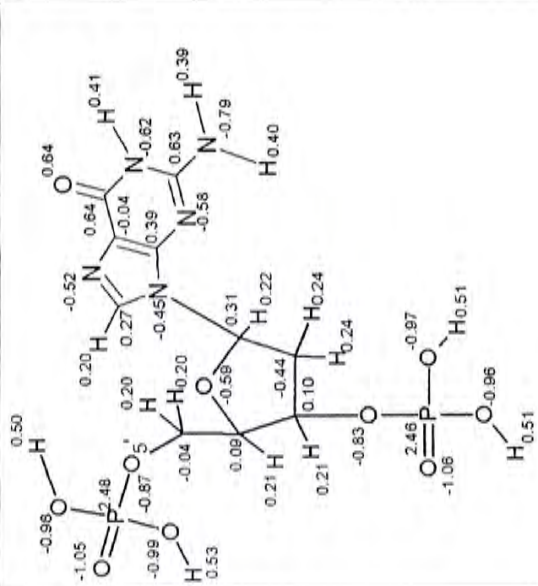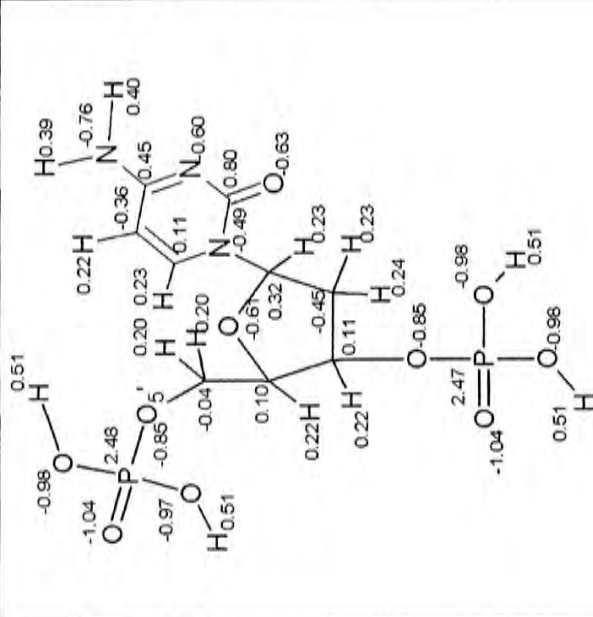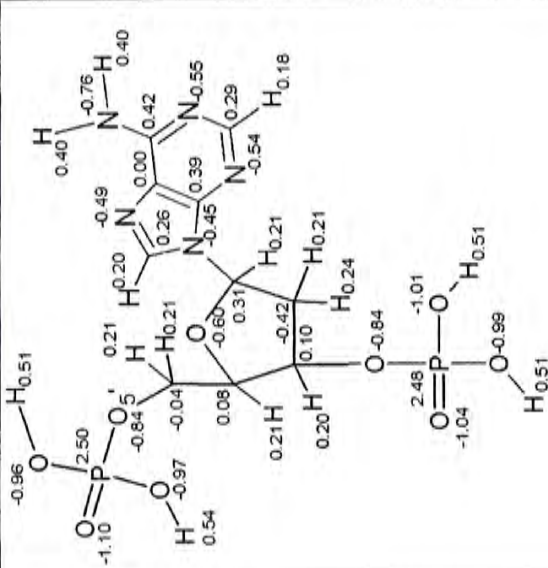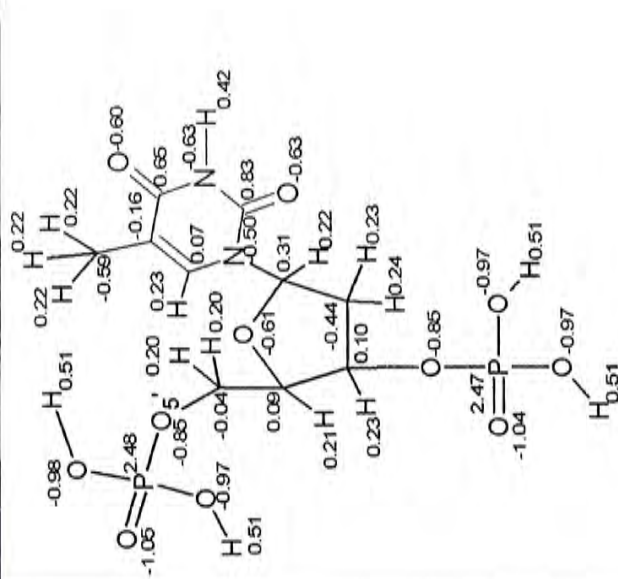
Charge distribution results are summarized in Tables 3.7 and 3.8. The details of charge distribution for each molecule (Table 3.7) reveal the location of atoms that became either electron deficient or electron rich. In Table 3.8, the charge distributions are represented in the form of the three functional components making up the DNA molecule, i.e. phosphate groups, sugar and base.

In guanine, phosphate groups accept a net of -0.35 electron and the base -0.25 electron whereas the sugar is +0.60 electron. It shows that one phosphate group and a base in guanine are electron rich whereas the sugar is electron deficient. The value in Table 3.8 implies that the backbone is electron deficient (net +0.23 charge). Charge distribution results of three other nucleotides are similar to that observed in guanine. Therefore, it is concluded that a base is electron rich and a backbone is electron deficient. Charge delocalizes on one phosphate group in the DNA backbone but not in the sugar. This result implies that the sugar cannot act as a charge sink.

3.1.5. Molecular Orbital

According to the theory of molecular orbital, HOMO represents the distribution and energy of the least tightly held electron in the molecule; whereas LUMO describes the easiest route to add an electron to a system. The HOMOs and LUMOs of the neutral nucleotides are presented in Table 3.9. The HOMOs show the pathway for removal of electron from the base, which is in full agreement with the NPA results presented in the last section. For the LUMO of guanine and cytosine, it is revealed that the easiest

31

Table 3.7

Charge distribution of the four nucleotides in their neutral states

Components	Net charge
Phosphate groups	-0.35
Sugar	0.60
Base	-0.23

Components	Net charge
Phosphate groups	-0.35
Sugar	0.60
Base	-0.25

Components	Net charge
Phosphate groups	-0.31
Sugar	0.56
Base	-0.25

Components	Net charge
Phosphate groups	-0.34
Sugar	0.60
Base	-0.26

32

Fig 3.7 Classification based on two different groups (base and backbone)
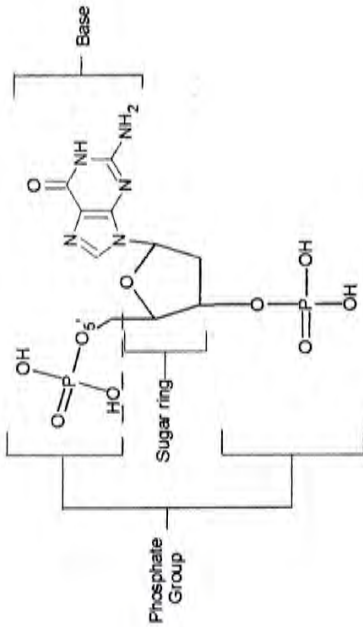
Fig 3.8 Classification based on three different groups (base, sugar, and phosphate groups)
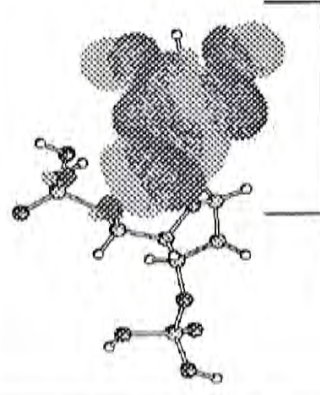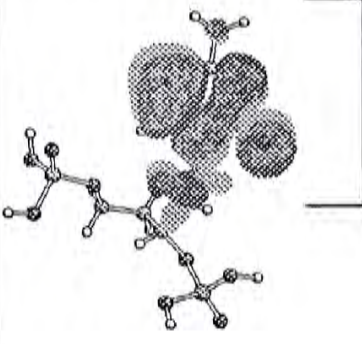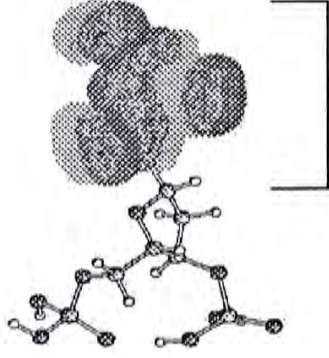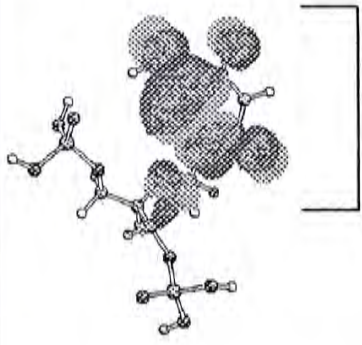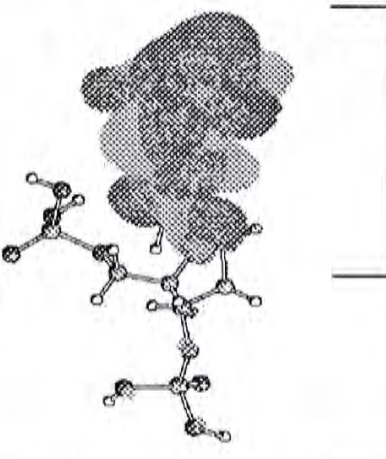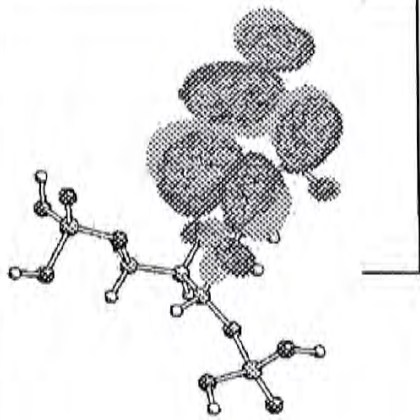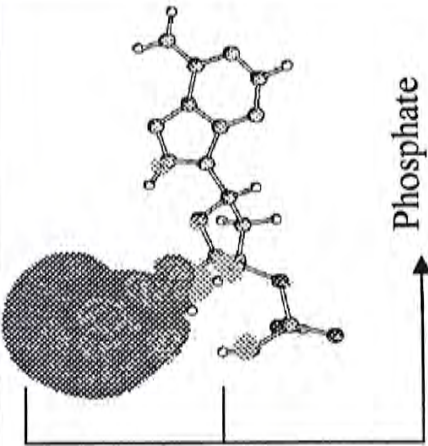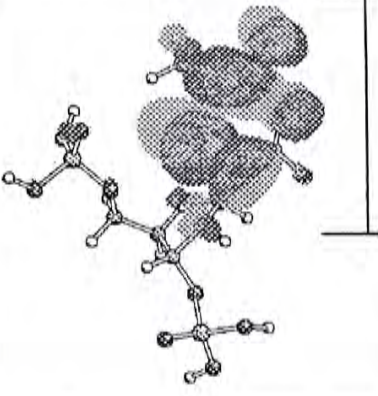
Table 3.8

Summary of the charge distribution of four different nucleotides (guanine, cytosine, adenine, and thymine) in their neutral states

	G	C	A	T
Phosphate Group	-0.35	-0.35	-0.31	-0.34
Sugar	0.60	0.60	0.56	0.60
Backbone (phosphate groups + sugar)	0.23	0.25	0.25	0.26
Base	-0.23	-0.25	-0.25	-0.26
Total	0.00	0.00	0.00	0.00

Table 3.9

Molecular orbitals of HOMO and LUMO of guanine, cytosine, adenine and thymine at their neutral states

route for adding an electron to the system is through their LUMOs in the base. However, an incoming electron prefers to localize on phosphate groups in neutral adenine (Table 3.9). Except for thymine, all other nucleotides show that their LUMO results are consistent with the results obtained from bond length and NPA data.

3.2. The Cationic State

The cation molecules were obtained through calculation of the optimized neutral molecules by removing an electron from the neutral nucleotides. In this section, Ionization potential (IP) results are reported together with the results of bond lengths, torsion angles and sugar puckering modes. After examining the structural changes, details of their charge distribution and molecular orbital are reported and compared with the results obtained from the respective neutral molecules. The last section presents a discussion of the chemical implication on DNA in the cationic state.

3.2.1. Ionization Potential

The vertical ionization potential (VIP), adiabatic ionization potential (AIP) and reorganization energy of all four nucleotides are summarized in Table 3.10. Since the reorganization energy is the energy difference between the VIP and the AIP, therefore guanine has the lowest VIP among the four nucleotides whereas the highest is found in thymine.

Table 3.10

AIP, VIP and Reorganization energy of DNA nucleotides

Nucleotide	AIP (eV)	VIP (eV)	Reorganization Energy (eV)
G	7.60	8.07	0.33
C	7.78	8.32	0.54
A	7.83	8.22	0.39
T	7.93	8.54	0.61

Table 3.11

Energy trends of four nucleotides

VIP	$T > C > A > G$
AIP	$T > A > C > G$
Reorganization Energy	$T > C > A > G$

Table 3.11 summarizes the VIP, AIP and reorganization energy trends for the four nucleotides. The trends of VIP and reorganization energy show agreement with the results of the VIP trend reported by Sevilla (33, 34, 38, 39), and that it solely accounts for energy changes without effecting large structure changes when an electron is removed. Based on this rationale, the data shows that it is easier to remove an electron from cytosine than adenine because it requires less energy to remove the electron and adjust the molecular structure. However, for AIP and VIP, thymine requires the most energy whereas guanine requires the least energy to remove an electron and to readjust its structure. This explains why guanine is found to be the most easily oxidized (13, 14, 17). In a cation molecule, the reorganization energy is energy releases to reorganize its structure to form a stable structure when an electron is removed. The trend of reorganization energy for the four nucleotides follows

$$T >> C > A > G$$

36

It shows that the structure of T is the most flexible when compared with other nucleotides and that G is the least flexible. This observation agrees with experimental findings (34) that thymine can release the most energy to stabilize its structure.

3.2.2. Bond length

In guanine, after an electron is removed, the greatest charge shifts takes place in the base (Table 3.18) and the corresponding bond lengths changes is shown in Fig 3.9. Due to the charge-density rearrangement, the bond lengths in the base strengthen or shorten accordingly. For example, the bond lengths of C2-N3 ($\Delta = 0.5$ Å), C4-C5 ($\Delta = 0.4$ Å), C5-C6 ($\Delta = 0.06$ Å), N7-C8 ($\Delta = 0.04$ Å) and N9-C1' (sugar ring) ($\Delta = 0.06$ Å) increase whereas the bond lengths of C2-N2 ($\Delta = 0.04$ Å), N3-C4 ($\Delta = 0.04$ Å), C5-N7 ($\Delta = 0.04$ Å) and C8-C9 ($\Delta = 0.03$ Å) decrease.

Charge delocalization is expected in the base because it is composed of either 5- and/or 6-membered ring molecules. From the above results, bond lengths increase and decrease alternatively within the base, which consists of single and double bonds. The same results are observed in other nucleotides in which the bond lengths of DNA-base rearranged due to the relocalization of charges in the system. Base becomes more flexible because charges mainly declocalize in cation molecules. Therefore, adjustment of bond lengths is possible because tangible damage to the integrity of the structure is minimized upon removal of an electron. The discussion in rearrangement of charge density is delayed to sections 3.2.6 and 3.2.7.

Note that for the glycosidic bond N9/N1-C1', which connects the sugar and the base, increases but no change is observed in its bond length when an electron is removed.

37

3.2.3. Backbone Torsion Angles

The backbone of nucleotides consists of seven torsion angles (α, β, γ, δ, ε, ζ, χ) with large degrees of freedom. Thus, nucleotides can adapt to different environments or conditions by adjusting their torsion angles correspondingly. In guanine, only small change is found in torsion angles of its backbone (Table 3.13). This result confirms that the backbone of guanine sustains little changes despite changes to its electronic structure. It implies that the degree of freedom of guanine is low when compared with other nucleotides, and its backbone shows little flexibility in adapting to changes in its electronic density. In cytosine, adenine and thymine, a similar but different pattern of data is revealed, i.e. one torsion angle is shifted outside the normal range for each of the nucleotide. The data also reveals that the backbone of cytosine is the most flexible with large degrees of freedom to cope with conformation rearrangement by adapting the change in its electronic state. In adenine and thymine, only one torsion angle change is observed for each nucleotide.

Thus, backbones of cytosine, adenine and thymine have similar degree of freedom and ranges for their torsion angles are similar. Because the level of flexibility is affected by the coupling between the base and the environment, backbone of these base have greater degrees of freedom. Among the three nucleotides, cytosine attained the greatest degrees of freedom.

Table 3.12

Change in the bond length in the base of each nucleotide when an electron is removed
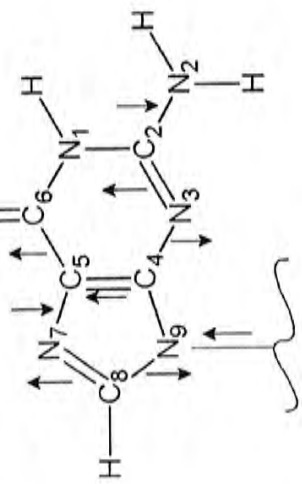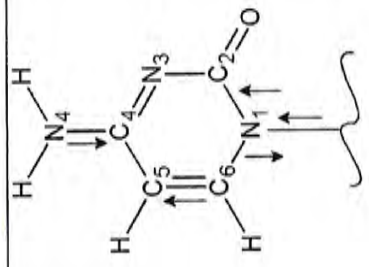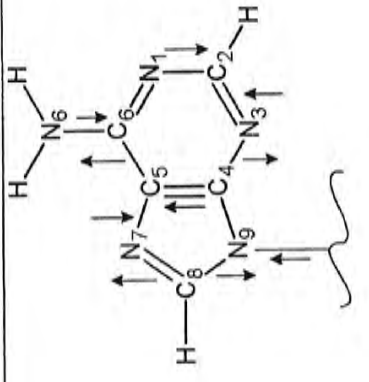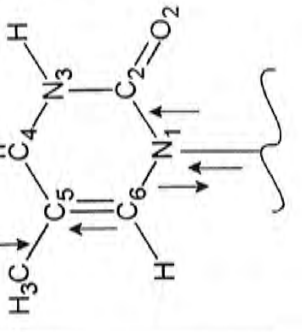
Cationic state (An electron remove from the system)			
G	C	A	T

Bond and the change in their bond lengths (Å)			
G	**C**	**A**	**T**
C_2-N_2 (Δ = 0.508Å↑) N_7-C_8 (Δ = 0.047Å↑)	N_1-C_2 (Δ = 0.053Å↑)	C_2-C_3 (Δ = 0.04Å↑) $N7$-$C8$ (Δ = 0.052Å↑)	N_1-C_2 (Δ = 0.057Å↑)
C_4-C_5 (Δ = 0.410Å↑) N_9-$C_{1'}$ (Δ = 0.058Å↑)	C_5-C_6 (Δ = 0.048Å↑)	C_4-C_5 (Δ = 0.04Å↑) N_9-$C_{1'}$ (Δ = 0.061Å↑)	C_5-C_6 (Δ = 0.063Å↑)
C_5-C_6 (Δ = 0.067Å↑)	N_1-$C_{1'}$ (Δ = 0.037Å↑)	C_5-C_6 (Δ = 0.03Å↑)	N_1-$C_{1'}$ (Δ =0.062Å↑)
C_2-N_2 (Δ = 0.042Å↓) C_5-N_7 (Δ = 0.043Å↓)	N_1-C_6 (Δ = 0.029Å↓)	N_1-C_2 (Δ = 0.038Å↑) C_6-N_6 (Δ=0.029Å↑)	N_1-C_6 (Δ = 0.067Å↓)
N_3-C_4 (Δ = 0.044Å↓) C_8-C_9 (Δ = 0.038Å↓)	C_4-N_4 (Δ = 0.030Å↓)	N_3-C_4 (Δ = 0.049Å↑) C_8-N_9 (Δ= 0.046Å↑)	C_5-C(methyl group) (Δ = 0.034Å↓)
		C_5-N_7 (Δ = 0.054Å↑)	

39

Table 3.13

Summary of calculated torsion angles and statistic analysis of the torsion angles derived from crystal structure for DNA backbone

Torsion Angle	Base Ref.*	G Cat	G Neu	C Cat	C Neu	A Cat	A Neu	T Cat	T Neu
A	270 - 330	268	289	46	314	299	286	307	313
B	130 - 220	178	170	118	183	247	236	233	167
Γ	20 - 80	52	50	50	56	58	53	73	56
Δ	70 - 180	107	106	131	135	87	103	143	138
E	160 - 270	204	209	158	196	212	249	209	202
Z	230 - 300	188	180	296	294	328	179	275	267
	150 - 210								
X	200 - 300	295	289	161	227	198	237	193	242

*Ref 52

The data in Table 3.14 shows that the difference of pseudo-rotation phase angles between neutral and cation molecule is around 2-7 degrees for guanine and cytosine. It confirms that removal of an electron has little impact on the conformations of their sugar ring. Compared with neutral and cationic state, their conformations are similar. Their puckering modes are almost the same when an electron is removed. In guanine and cytosine, their structures are stable with relatively low reactivity energy for these puckering modes (Fig. 3.10).

Table 3.14

Sugar conformation (pseudo-rotation phase angle and puckering mode)
in the neutral and the cationic states

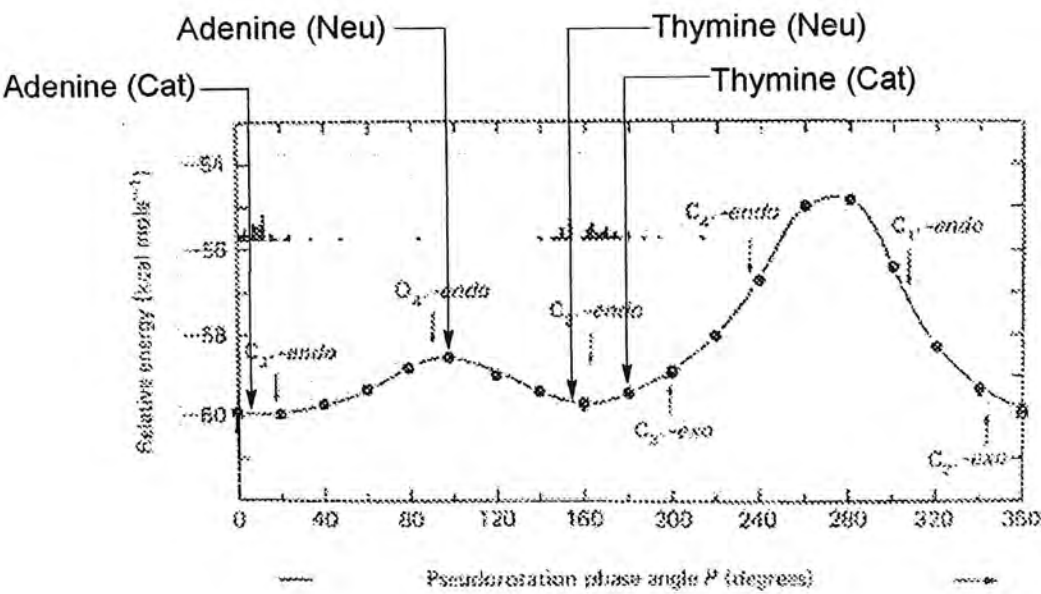|	G		C		A		Thy	
State	Cat	Neu	Cat	Neu	Cat	Neu	Neu	Cat
Pseudo-rotation phase angle, P	325	327	139	146	14	100	156	180
Puckering Mode	^1_2T	^1_2T	$\%^2_1T/_1E$	^2_1T	^3E	$\%^0E/^0_1T$	$\%^2E/^2_1T$	^2_3T

Fig 3.10 Energy of sugar conformation of adenine and thymine in both neutral and cationic states

41

When an electron is removed, large change in the pseudo-rotation phase angle and the puckering mode are observed. In the neutral state, its puckering mode falls between ^0E and ^0_1T and its conformation is nearly $O_{4'}$-endo. After removing an electron, the sugar adopts the ^3E puckering mode and its conformation becomes $C_{3'}$-endo because the $O_{4'}$-endo conformation is less stable. In thymine, the pseudo-rotation phase angle decreases by $24°$ and the sugar conformation change from the south to near the $C_{2'}$-endo. When compared with its neutral state, the energy is relatively low in the cation molecule. The same result is observed in adenine and thymine whereby both of their sugar rings are lower in energy in the cation molecules. Moreover, their puckering modes are also disposed nearly opposite to each other as shown in Fig 3.11 (b), the pseudo-rotation phase angle diagram of the furanose ring.

3.2.5.   Charge Distribution

When an electron is removed from a nucleotide, a molecule has an overall $+1$ charge. In guanine, the base accounts for the loss of -0.86 e^- whereas the source of the balance of -0.14 e^- (see Table 3.11) is from the backbone. This result shows that nearly 80% of the electronic charge is removed from the base of DNA nucleotide. From the results in Table 3.15 and 3.16, the greatest charge shift is observed in atoms N2, N3, O4, C5, O6, N7, C8 in the base. Similar observations were made for cytosine, adenine and thymine whereby > 80 % of electronic charge is lost from the base after removing an electron (Table 3.18). These data show that the ionization potential of a base is lower than that of a backbone because the base is readily oxidize. The results observed here is in agreement with work done by other groups (34, 25) whereby it has been shown that charges tend to localize in the 6 and/or 5-membered rings in DNA nucleotides. In total
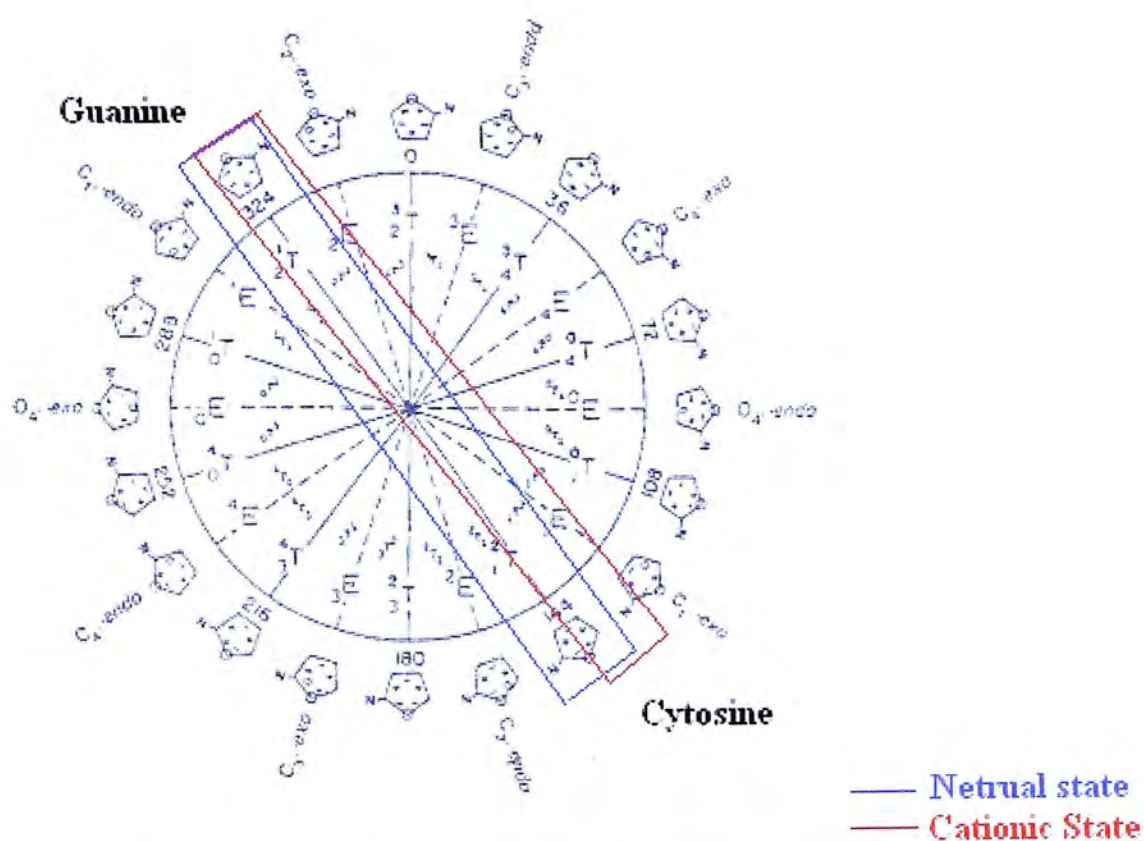
Fig 3.11 (a)   Sugar puckering modes in guanine and cytosine at the neutral and the cationic states
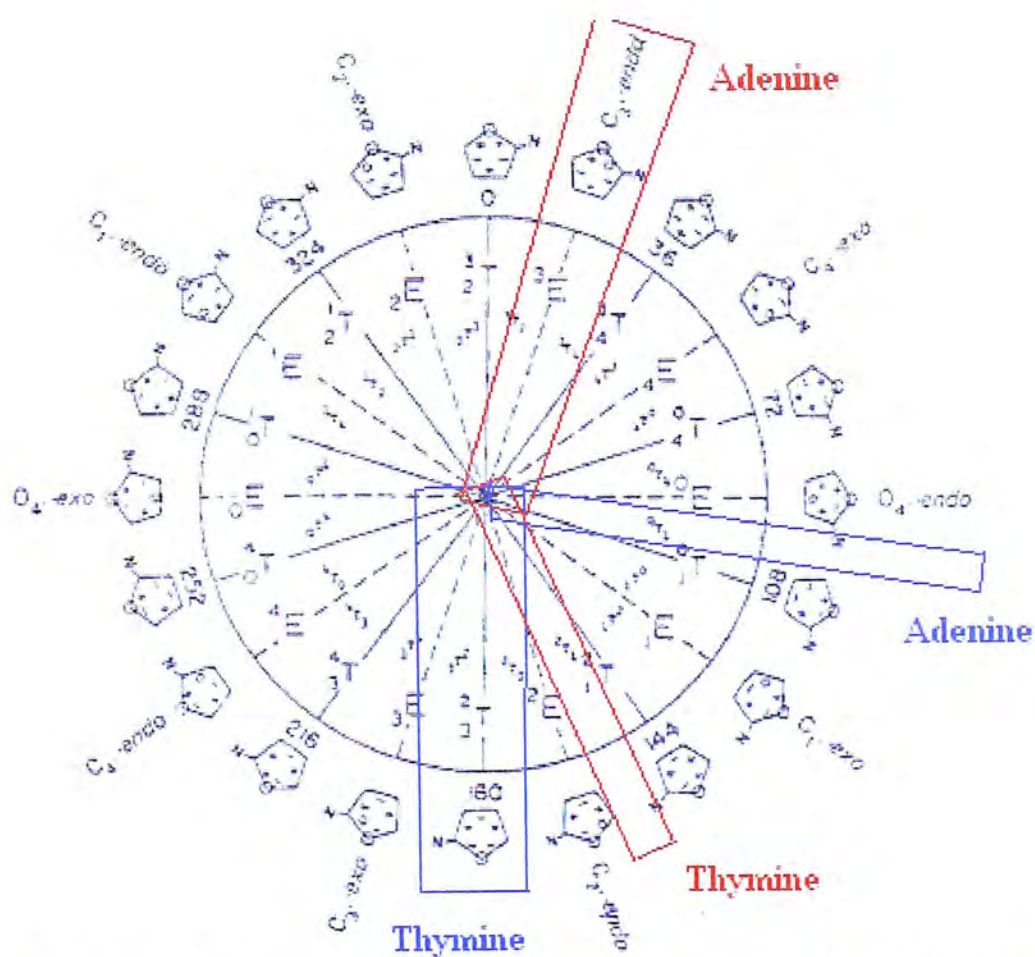
Fig 3.11 (b)   Sugar puckering modes in adenine and thymine at the neutral and the cationic states

43

Table 3.15

Charge distribution of guanine and cytosine in the neutral and the cationic states

	Neu		Cat	
G				
	Components	Net charge	Components	Net charge
	Phosphate groups	-0.35	Phosphate groups	-0.35
	Sugar	0.60	Sugar	0.60
	Base	-0.23	Base	0.63
C				
	Components	Net charge	Components	Net charge
	Phosphate groups	-0.35	Phosphate groups	-0.27
	Sugar	0.60	Sugar	0.67
	Base	-0.25	Base	0.60

Table 3.16

Charge distribution of adenine and thymine in the neutral and the cationic states

	Neu			Cat	
A					
Components	Net charge		Components	Net charge	
Phosphate groups	-0.31		Phosphate groups	-0.26	
Sugar	0.56		Sugar	0.64	
Base	-0.25		Base	0.62	
T					
Components	Net charge		Components	Net charge	
Phosphate groups	-0.34		Phosphate groups	-0.28	
Sugar	0.60		Sugar	0.70	
Base	-0.26		Base	0.58	

Table 3.17

Summary of the charge distribution of four different nucleotides (guanine, cytosine, adenine, and thymine) in their neutral and cationic state

	G			C			A			T		
	Neu	Cat	Δ*	Neu	Cat	Δ*	Neu	Cat	Δ*	Neu	Cat	Δ*
Phosphate Group	-0.37	-0.27	0.10	-0.35	-0.27	0.08	-0.31	-0.26	0.05	-0.34	-0.28	0.06
Sugar ring	0.60	0.64	0.04	0.60	0.67	0.07	0.56	0.64	0.08	0.60	0.70	0.10
Backbone (Phosphate group + sugar ring)	0.23	0.37	0.14	0.25	0.40	0.15	0.25	0.38	0.13	0.26	0.42	0.16
Base	-0.23	0.63	0.86	-0.25	0.60	0.85	-0.25	0.62	0.87	-0.26	0.58	0.84
Total	0.00	1.00	1.00	0.00	1.00	1.00	0.00	1.00	1.00	0.00	-1.00	1.00

* The difference between the neutral and the cationic state

Table 3.18

Atoms with the greatest charge shift in each nucleotide

	G**	C**	A**	T**
Greatest charge shift atom	N2, N3, N7 C5, C8 O4, O6	N1 C5, C6 O2, O4	N1, N3, N6, C2, C5, C8	N1, N3, N4 C5 O2

** The charge shift takes place in the base.

~ 20 % of electron charge is found on phosphate, therefore it has a less important role in structure stabilization and we did not find any meaningful changes in the charge density of sugar (Table 3.17). A summary of charge distribution in each nucleotide is given in Table 3.17.

3.2.6. Molecular Orbital

The HOMO and the LUMO results in the cationic state for all nucleotides are presented in Tables 3.19 and 3.20.

The LUMO data shows that all cation molecules behave similarly. Because electron density of an additional electron is expected to mainly localizes on the base when compared with result of neutral molecules, discussed in section 3.1.5, therefore the base is the preferred site to accommodate electron rearrangement in its neutral state to form a cation molecule. The LUMOs demonstrate the pathway for accepting an additional electron. As discussed in section 3.14, the first electron is removed from a base.

The HOMO results presented in section 3.1.5 also show that the first electron is likely to be removed from the base. Therefore, the HOMOs in the cationic state also show that it is the site for a departing electron, but this would be the second departing electron. In guanine (Table 3.21), HOMOs of cation molecules show that the second electron is also likely to be removed from the base. Based on the data presented in Tables 3.19 and 3.20, similar patterns were observed for the other three nucleotides.

3.2.7. Summary

According to the ionization potential, guanine has the lowest energy and is the easiest to be oxidized whereas thymine has the highest IP. Base in a nucleotide has the lowest potential among the different components in each nucleotide. Based on charge distribution obtained form NPA studies (3.15) and molecular orbital result (3.16), charge would most likely depart from a base when an electron is removed.

Charge density of a base decreases (N2, N3, O4, C5, O6, N7) after adding an electron. Due to the greatest charge shifts takes place in the base, the bond lengths of the base sustain the largest change when compared with the backbone or the sugar. Charge redistribution mainly takes place in the base of nucleotide rendering the base to take on electrophilic character and that bond lengths in base strengthen and shorten due to changes in charge density of each atom. In the base, the bond lengths C2-N2, C4-C5, C5-C6, N7-C8, N9-C1' increase whereas that of C2-N2, N3-C4, C5-N7, C8-C9 decrease.

In the sugar, the charge density is observed to remain almost unchanged for the different nucleotides because structures can be stabilized through the changes in puckering modes. For guanine and cytosine, the observation is made that the sugar puckering modes are symmetrically disposed opposite to each other both in their neutral and cationic states. In adenine and thymine, the same behavior is found for their sugar puckers in their cation molecules but not in the neutral molecules. In the backbone, guanine has the lowest degrees of freedom whereas cytosine commands the greatest freedom among the four nucleotides.

Table 3.19

The molecular orbital of HOMO and LUMO of guanine and cytosine
at the neutral and the cationic state
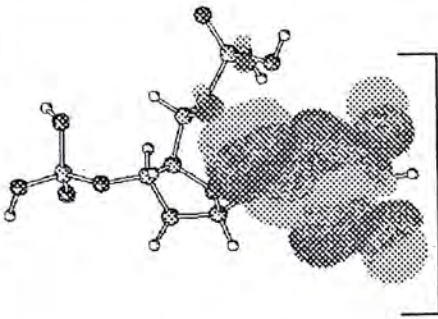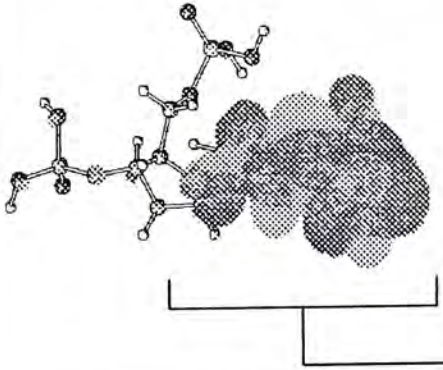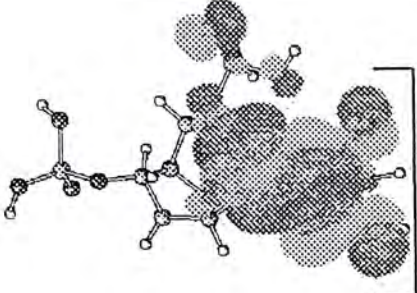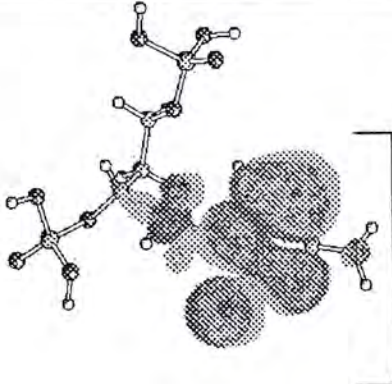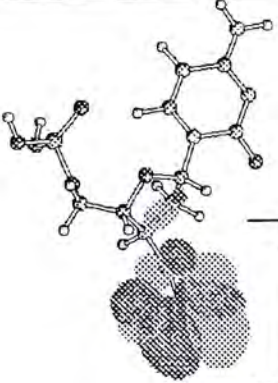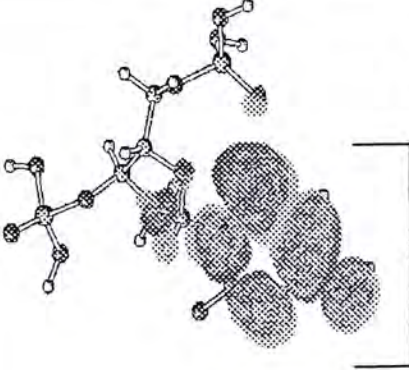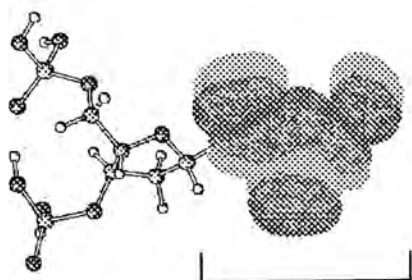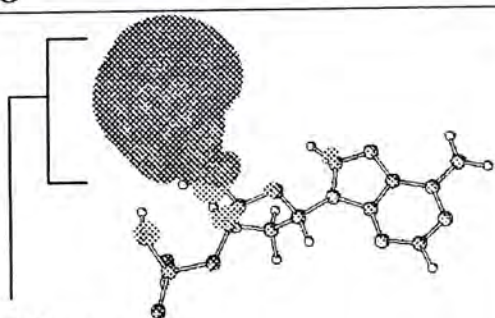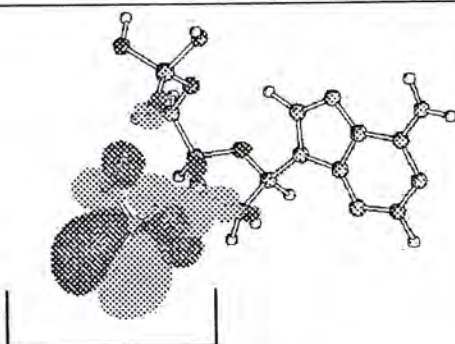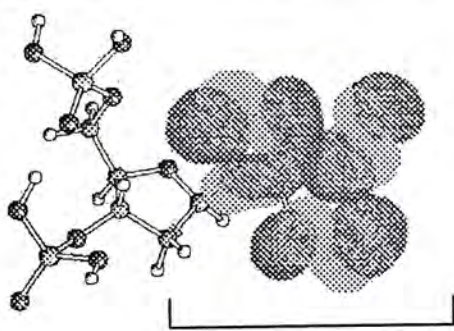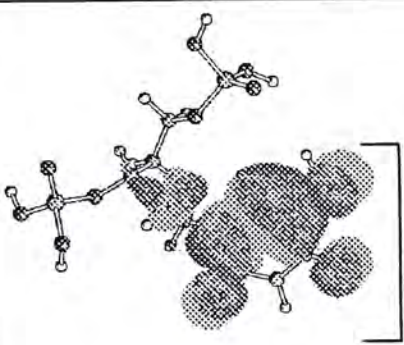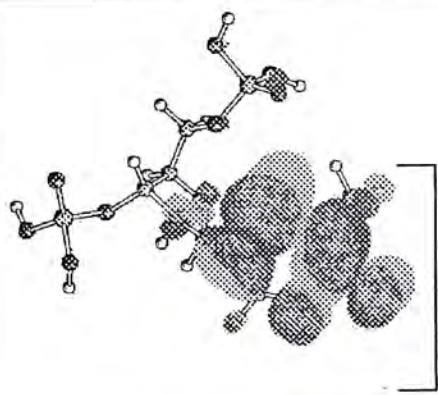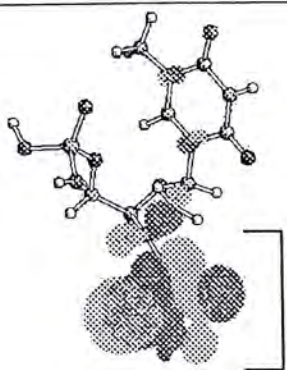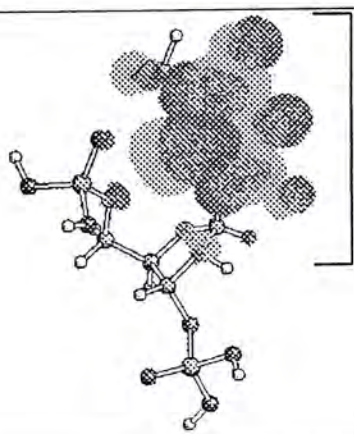
	HOMO	LUMO
G (neu)	Base	Base
G (cat)	Base	Base
C (neu)	Base	Base
C (cat)	Phosphate group (P3')	Base

Table 3.20

The molecular orbital of HOMO and LUMO of adenine and thymine
at the neutral and cationic state

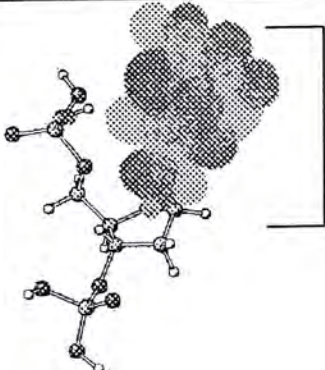|	HOMO	LUMO
A (neu)	base	Phosphate group (P5')
A (cat)	Phosphate group (P3')	base
T (neu)	base	base
T (cat)	Phosphate group (P3')	base

Results in this project show that the reactivity of guanine is the lowest among the four nucleotides because it is the most stable and is least likely to sustain changes. The more stable a structure is, the more stable the molecule remains. Previous studies (6 – 12) show that the sites of G, GG and GGG are most easily damaged, which imply that guanines have the least ability to sustain damages to its structure. In cytosine, its backbone has the largest degree of freedom and may constitute a pathway to assist the molecule to adapt to changes. For adenine and thymine, the backbone and the sugar ring can play important complementary roles in structure stabilization.

3.3. Anionic State

In this section, we will begin the discussion with the electron affinity (EA) results. This is followed by a discussion of data on bond lengths, torsion angles and sugar puckering modes. After investigating structural changes, the details of the charge distribution and molecular orbital (HOMO and LUMO) for each molecule are reported and compared with the results obtained in the neutral molecules.

3.3.1. Electronic Affinity

The electron affinity (EA) is the minimum energy release when an electron is added to a molecule. A study of the electron affinity can reveal which nucleotide is the easiest and which one is the most difficult to accept an additional electron (58). The Adiabatic electron affinity (AEA), vertical electron affinity (VEA) and reorganization energies for the four nucleotides are summarized in Table 3.21.

Table 3.21

AEA, VEA and Reorganization energy of DNA nucleotides (eV)

Nucleotide	AEA (eV)	VEA (eV)	Reorganization Energy (eV)
G	-0.23	-0.02	-0.21
C	-0.37	-0.10	-0.27
A	-0.64	-0.20	-0.44
T	-1.72	-0.22	-1.50

The reorganization energy is the difference between AEA and VEA, and their trends together with that of the reorganization are shown in Table 3.22. It is concluded that guanine releases the least energy whereas thymine releases the most energy upon adding an electron. The data further reveals that thymine is the easiest to gain an electron to form an anion molecule and in the process releases the most energy to achieve structure stabilization. The reorganization energy has a similar trend when compared with its IP and EA, with thymine releases the most reorganization energy when an electron is added.

Table 3.22

Trends of AEA, VEA and Reorganization energy of four nucleotides

AEA	G > C > A > T
VEA	G >> G > A > T
Reorganization Energy	T >>> A > C > G

3.3.2. Bond lengths

When an electron is added, bond lengths also change and these results are reported in Table 3.23. In guanine and adenine, there is essentially no change in the bond lengths. When the results are compared with their neutral molecule, the additional electron is

not found to delocalize on the base, which suggests that other methods is at play to adapt the changes.

In cytosine, the bond lengths of N3-C4 ($\Delta = 0.03$ Å), C4-N4 ($\Delta = 0.04$ Å) and N_1-$C_{1'}$ ($\Delta = 0.02$ Å) increase and the bond length of C4-C5 ($\Delta = 0.03$ Å) decreases. Except for the gylcosylic bond (N_1-$C_{1'}$), all changes in bond length were found in the base. No change is observed in the sugar or in phosphate groups. The details of the charge distribution and molecular orbital are discussed in section 3.3.5 and 3.3.6.
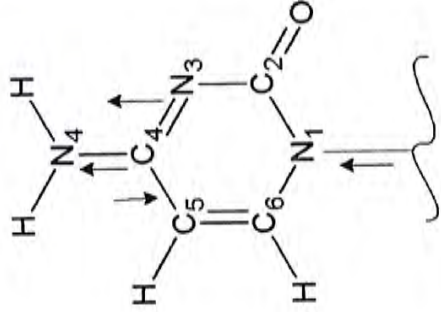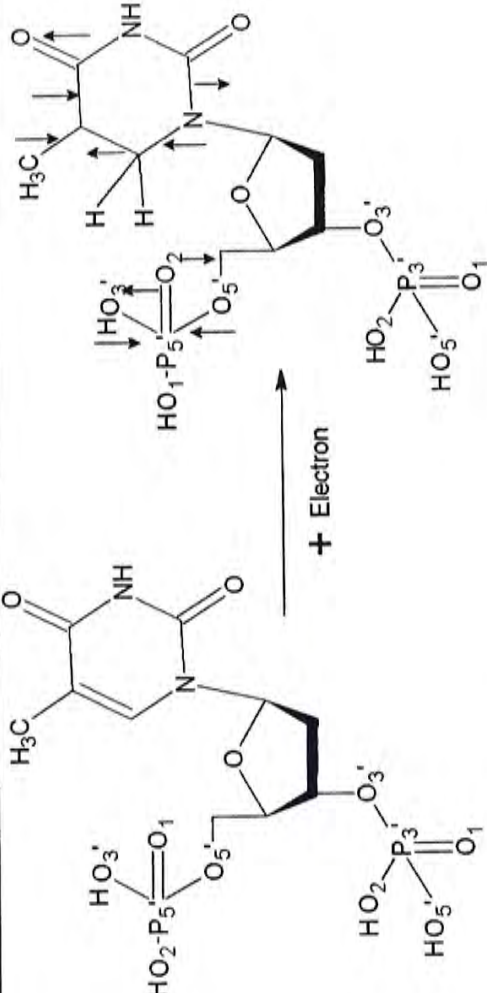
In thymine, the result is completely different from the other three nucleotides. After adding an electron, an intra-molecular proton (H) transfer process was detected in addition to the changes occurring in bond lengths in the molecule. A proton (H), attached to the O2 oxygen in the P5' phosphate group is transferred to C5 in the base. The bond lengths of N1-C6 ($\Delta = 0.09$ Å), C5-C6 ($\Delta = 0.14$ Å), P-O1 ($\Delta = 0.06$ Å) and P-O5' ($\Delta = 0.08$ Å) increase and those of N1-C2 ($\Delta = 0.03$ Å), C4-C5 ($\Delta = 0.03$ Å), C5'-O5' ($\Delta = 0.03$ Å) and P-O1' ($\Delta = 0.06$ Å) decrease. Change in bond lengths of the base is due to the intra-molecular proton transfer reaction, which causes change in the charge density of the system.

3.3.3. Torsion Angles of Backbone

The torsion angles of all four neutrals and anion nucleotides are summarized in Table 3.24. The difference in torsion angles is small and all the torsion angles fall within their ranges determined from experimental data. With anionic adenine being the only exception, its torsion angle ζ reveals a large difference when compared with its neutral

Table 3.23

Change in the bond lengths in the base of each nucleotide when an electron is added

Anionic state (an electron addition to the system)			
G	C	A	T

G: Remain also unchanged

C:

N$_3$ – C$_4$ (Δ = 0.033 Å ↑)
N$_4$ – C$_4$ (Δ = 0.039 Å ↑)
N$_1$ – C$_{1'}$ (Δ = 0.026Å ↑)
C$_4$ – C$_5$ (Δ = 0.032Å ↓)

A: Remain also unchanged

T:

+ Electron

N$_1$ – C$_6$ (Δ = 0.095 Å ↑)
C$_5$ – C$_6$ (Δ = 0.141 Å ↑)
P – O$_1$ (Δ = 0.604 Å ↑)
P – O$_{5'}$ (Δ = 0.810 Å ↑)

N$_1$ – C$_2$ (Δ = 0.033 Å ↓)
C$_4$ – C$_5$ (Δ = 0.030Å ↓)
C$_{5'}$ – O$_{5'}$ (Δ = 0.028Å ↓)
P – O$_{1'}$ (Δ = 0.062Å ↓)

molecule. It shows that the backbone of the adenine anion is upon adding an electron.

3.3.4. Sugar Ring Puckering Mode

The data in Table 3.25 shows that the pseudo-rotation phase angle and puckering modes of the neutral and anionic states are similar in guanine and cytosine. Conformations of guanine and cytosine remain unchanged in the $_2^1T$ and $_1^2T$ respectively after adding an election to the neutral molecule. The puckering mode of guanine is C_1-endo and that of cytosine is C_1-exo. In guanine and cytosine, the impact on the sugar conformation is small and their sugar rings remain symmetrically align on the opposite side to each other in the pseudo-rotation phase cycle of the furanose ring (see Fig 3.13 (a)). In adenine and thymine, the difference in the pseudo-rotation phase angles between the neutral and the anionic states is small. The conformation of adenine is between ^0E and $_1^0T$ and its energy is close to its neutral molecule (Fig 3.12) whereas the sugar conformation is near C_1-exo. The conformation of thymine is around C_2-endo upon adding/removing an electron. In adenine and thymine, the sugar conformations were altered when an electron is added to their respective neutral molecules (see Fig 3.13 (b)). Thus, this result suggests structural stabilization of nucleotide in the anionic state cannot solely rely on adjustment of the sugar conformation.

Table 3.24

Results of all torsion angles in backbone of DNA and the statistic results of the torsion angles of crystal structure of DNA.

Torsion Angle	Base Ref.*	G Neu	G An	C Neu	C An	A Neu	A An	T Neu	T An
α	270-330	289	293	314	307	286	290	313	337
β	130-220	170	158	183	180	236	**241**	167	146
γ	20-80	50	52	56	50	53	49	56	47
δ	70-180	106	104	135	129	103	112	138	148
ε	160-270	209	200	196	198	249	244	202	196
ζ	230-300	180	180	294	297	179	299	267	269
	150-210								
χ	200-300	289	286	227	228	237	226	242	236

*Ref. 52

Table 3.25

Sugar conformation (pseudo-rotation phase angle and puckering mode)
at their neutral and anionic states

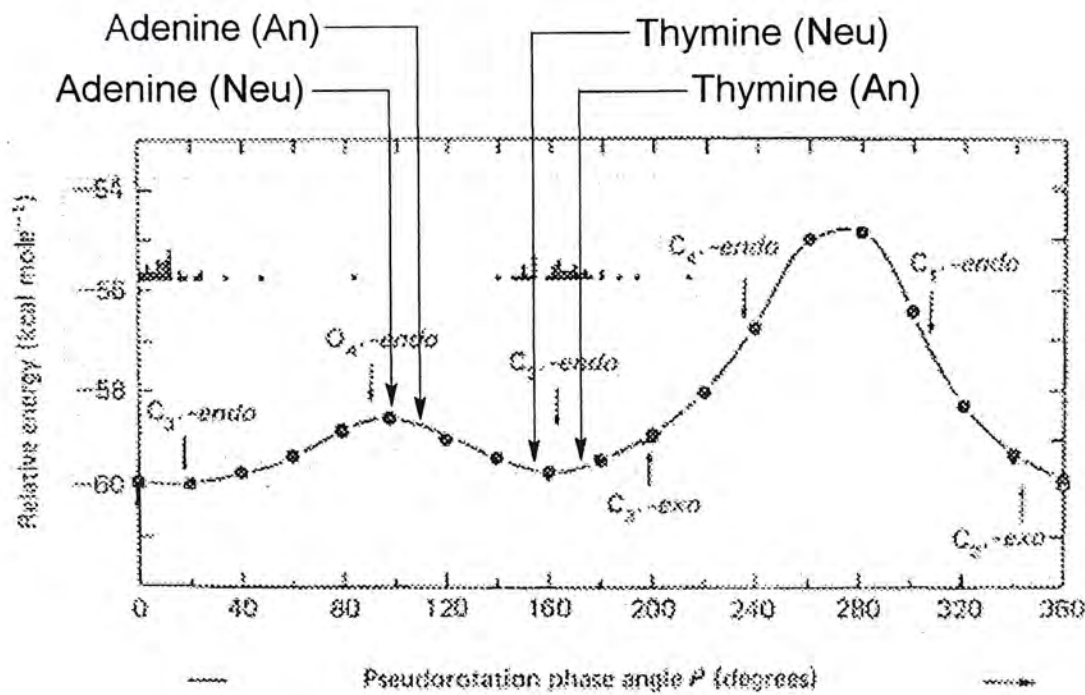|	G		C		A		T	
State	Neu	An	Neu	An	Neu	An	Neu	An
Pseudo-rotation phase angle, P	327	328	146	140	100	112	156	174
Puckering Mode	^1_2T	^1_2T	^2_1T	^2_1T	$\%^0E/^0_1T$	$_1E$	$\%^2E/^2_1T$	$\%^2_3T/^2E$

Fig 3.12 Energy of sugar conformation of adenine and thymine at the neutral and the
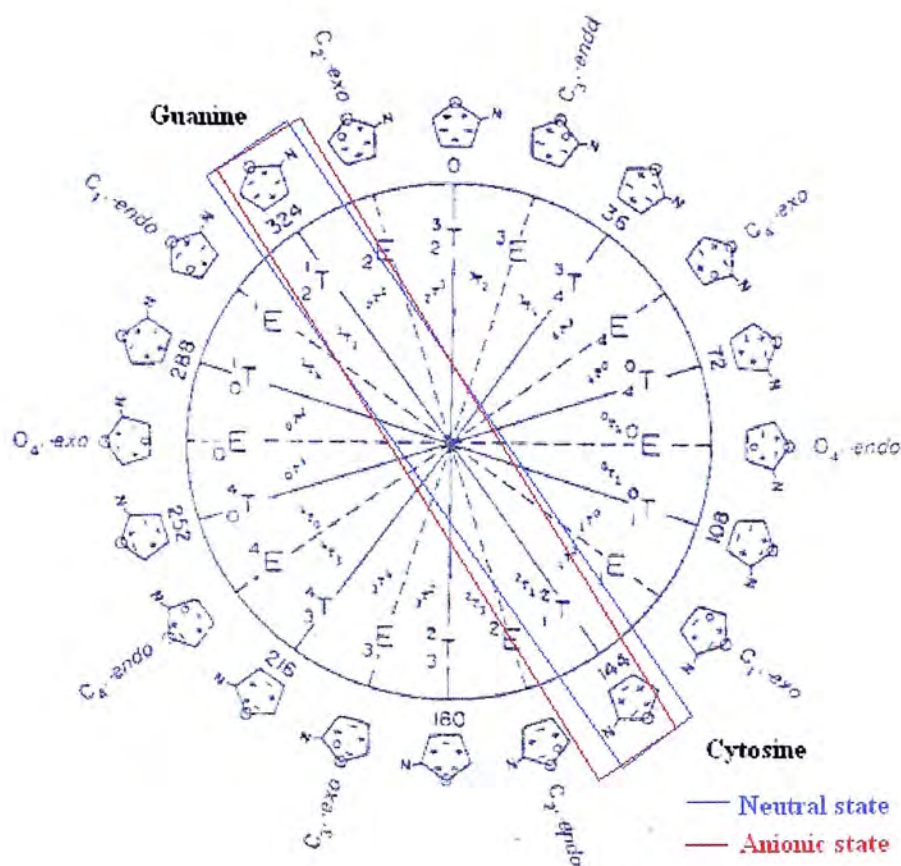anionic states

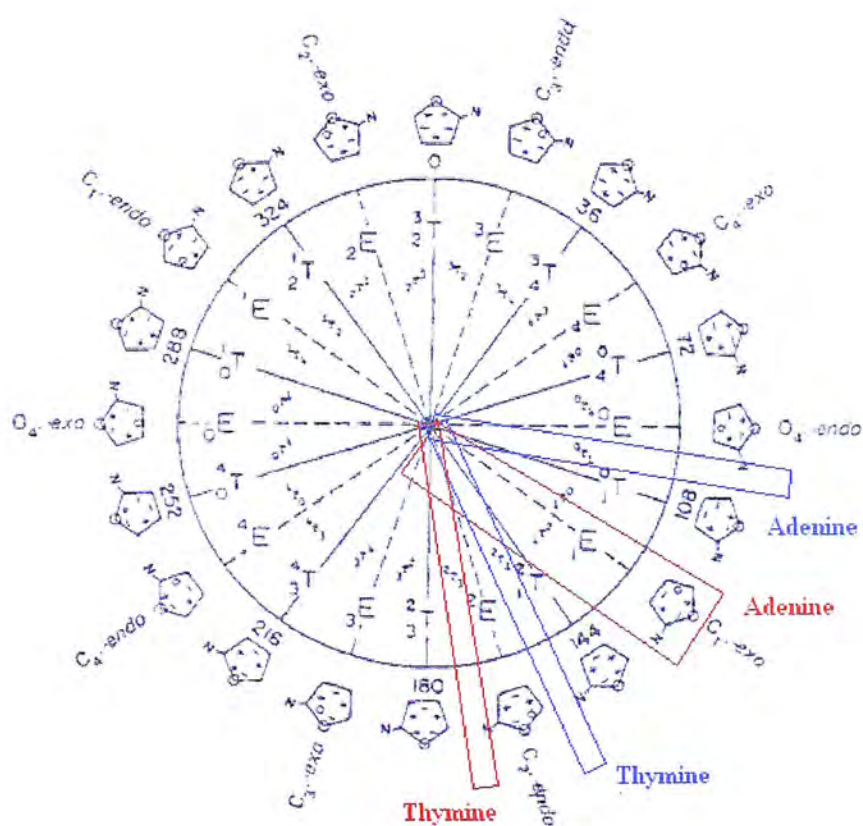Fig 3.13 (a) Sugar puckering modes guanine and cytosine at the neutral and the anion molecules

Fig .313 (b) Sugar puckering modes in adenine and thymine in the neutral and the anion molecules

3.3.5. Charge Distribution

When an electron is added to a nucleotide, the molecule carries an overall -1 charge. In guanine, the base accounts for -0.76 of the excess charges, and the balance (-0.24) is found in the backbone (Table 3.26 and 3.27). For cytosine, the base accounts for -0.75 excess charges, and the backbone carries the balance of -0.25 (Table 3.26 and 3.27). Considering the location of excess charges, it shows that 75% electron flows to the base and only 25% flows to the backbone (Table 3.28). When compared with their neutral molecules, percentage change of charge shifts in the base and the backbones are around 50 % for each component. This means that excess charge exerting on guanine and cytosine is distributed almost evenly between a base and a backbone.

In Table 3.29, the greatest charge shifts in guanine are observed to take place on the N1, C2, N2, H2 and O6 atoms in the base and P3' and O5' atoms connecting with P3'in the backbone. Because 50% of excess charges is located in the base, the atoms with the greatest charge shift in the base participate in H-bonds between the base pair of guanine and cytosine. The remaining excess charges are localized in the phosphate group (P3') on the backbone. Therefore, both the base and the P3' phosphate group can act as charge sinks and play important roles in structure stabilization after addition of an electron. Sugar did not show any participation in the structure stabilization process. The result for cytosine (Table 3.26, 3.28) reveals similar result of guanine. However, the excess charges are localized on P5' and not on P3'. In adenine, the base accounts for -0.37 excess charge whereas the backbone carries the balance of -0.63 charges. A comparison with its neutral molecule shows that 12 % of excess electronic charge was found to localize on the base and the remaining 88% on the backbone (Table 3.27, 3.28). The greatest charge shifts is observed on the P5' phosphate atom and the O1' and O2'

oxygen atoms, which are both bonded to P5' (Table 3.29). Therefore, the phosphate backbone plays an important role in the structural stabilization process.

In thymine, the base accounts for -0.26 of the excess charges, and the backbone carries -0.74 charge (Table 3.27 and 3.28). In short, between 80 - 100 % of excess electronic charges is localized on the backbone. A proton in the base transfers from the P5' phosphate group to the C5 atom in the base when an electron is added (Table 3.27 and 3.28). Since excess charge distributes mainly in the phosphate group, the backbone of anionic adenine and thymine are important components for localization of excess charges. From the percentage change of excess charge in each component, it is concluded that phosphate groups are better charge sinks in adenine and thymine. There is no evidence demonstrating that the sugar participates in the charge-sharing scheme as charges on the sugar remain unchanged when an electron is added.

3.3.6. Molecular Orbital

The results obtained for the HOMOs and the LUMOs of four anion nucleotides are presented in Tables 3.30 and 3.31. Accordingly, the LUMO of neutral molecules (section 3.1.5) shows that an additional electron is most likely to be add through the base for guanine, cytosine and thymine because the electron density of the lowest energy anti-bonding orbital is mainly located in the base. For the LUMO of the neutral adenine, the electron density of additional electron is predicted to be localized mainly on the P3' phosphate group.

Table 3.26

Charge distribution of guanine and cytosine in the neutral and the anionic states

	Neu		An	
G				
	Components	Net charge	Components	Net charge
	Phosphate groups	-0.35	Phosphate groups	-0.81
	Sugar	0.60	Sugar	0.56
	Base	-0.23	Base	-0.76
	Components	Net charge	Components	Net charge
	Phosphate groups	-0.35	Phosphate groups	-0.79
	Sugar	0.60	Sugar	0.54
	Base	-0.35	Base	-0.75

61

Table 3.27

Charge distribution of adenine and thymine in their neutral and anionic states

	Neu		An	
A				
	Components	Net charge	Components	Net charge
	Phosphate groups	-0.31	Phosphate groups	-1.16
	Sugar	0.56	Sugar	-0.53
	Base	-0.25	Base	-0.27
T				
	Components	Net charge	Components	Net charge
	Phosphate groups	-0.34	Phosphate groups	-1.31
	Sugar	0.60	Sugar	0.57
	Base	-0.26	Base	-0.26

Table 3.28

Summary of the charge distribution of all neutral and anion nucleotides (guanine, cytosine, adenine, and thymine)

State	Gua			Cyt			Ade			Thy		
	Neu	An	Δ	Neu	An	Δ	Neu	An	Δ	Neu	An	Δ
Phosphate Group	-0.35	-0.80	-0.45	-0.35	-0.79	-0.44	-0.31	-1.16	-0.85	-0.34	-1.31	-0.97
Sugar ring	0.60	0.56	-0.04	0.60	0.54	-0.06	0.56	0.53	-0.03	0.60	0.57	-0.03
Backbone (Phosphate group + sugar ring)	0.23	-0.24	-0.47	0.25	-0.25	-0.50	0.25	-0.63	-0.88	0.26	-0.74	-1.00
Base	-0.25	-0.76	-0.51	-0.25	-0.75	-0.50	-0.25	-0.37	-0.12	-0.26	-0.26	0.00
Total	0.00	-1.00	-1.00	0.00	-1.00	-1.00	0.00	-1.00	-1.00	0.00	-1.00	-1.00

Table 3.29

Atoms with the greatest charge shift in guanine, cytosine, adenine and thymine

The greatest charge shift atoms	G	C	A	T
Base	N1, N2, C2 O6 H2	N3, N4 C4, C6 O2	--	C5, C6
Phosphate backbone	P3', O5'	P5'	P (5') H (in P5') H (in P3')	O3' (in P5')

The HOMOs of the anionic guanine and cytosine (see Table 3.31) show that the electron density of the outer-most electron is localized evenly on the phosphate group and on the base. Since the results of anions' HOMOs show where the additional electron will locate, they are expected to be consistent with that of their respective LUMOs in the neutral molecule. For thymine, the HOMO shows that the charge density of an outer-most electron localizes mainly on the base and partially on the P5' phosphate group. However, the HOMO result of adenine is different from all three other nucleotides, in which the charge density of an outer-most electron is found to localize almost exclusively on the phosphate group. This result agrees with the charge distribution in an anionic molecule.

The results of the HOMO of all four anion nucleotides (Table 3.30 and 3.31) shows where the first electron will localize, and the LUMO of all four anion nucleotides show where the second electron localizes in the molecule. Accordingly, based on results and the discussion present in section 3.1.5, the electron density of the first electron is expected to evenly localize on the base and on the phosphate group in guanine and cytosine. The LUMO of anion guanine and cytosine shows that electron distribution for the second electron is similar to that of the first electron. For adenine, a large portion of the electron density of the first electron is localized in the P3' phosphate and the second electron is mainly localized on the base. For thymine, the charge density of the first electron mainly localizes on the base whereas the second electron is expected to localize on the phosphate groups.

Table 3.30

The molecular orbital of HOMO and LUMO of guanine and cytosine
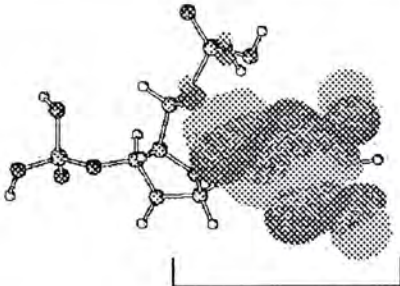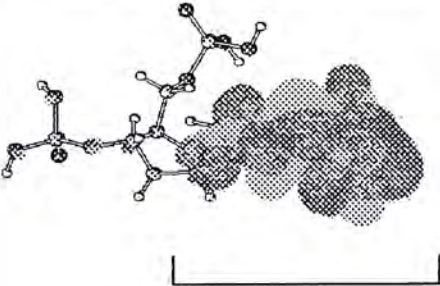at the neutral and the anionic states
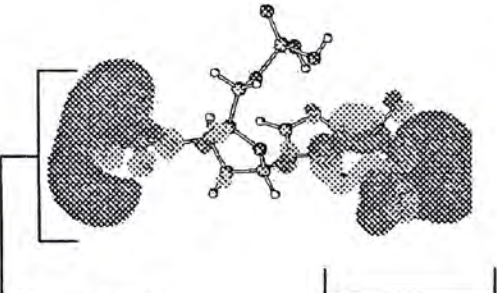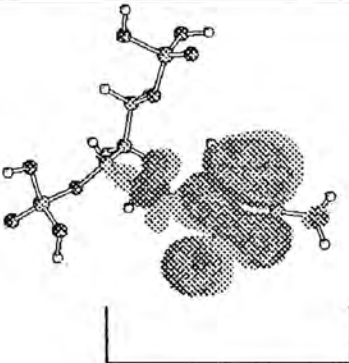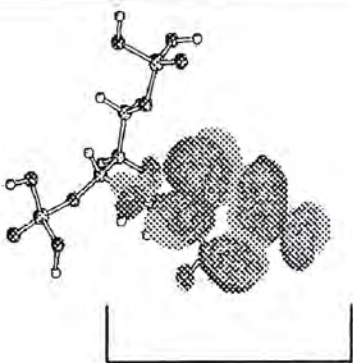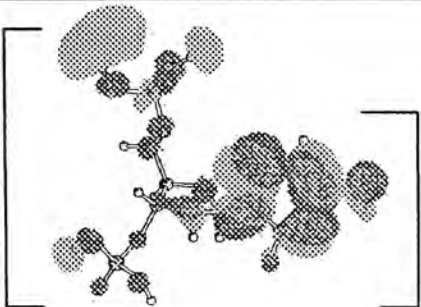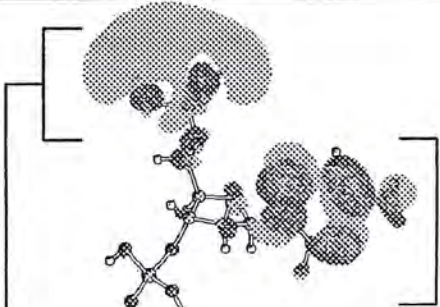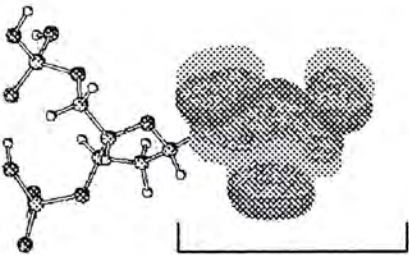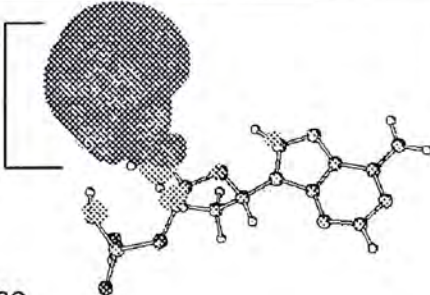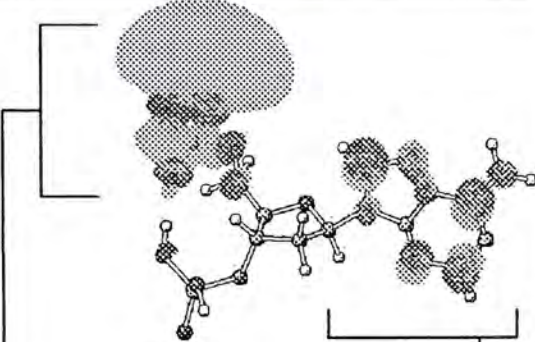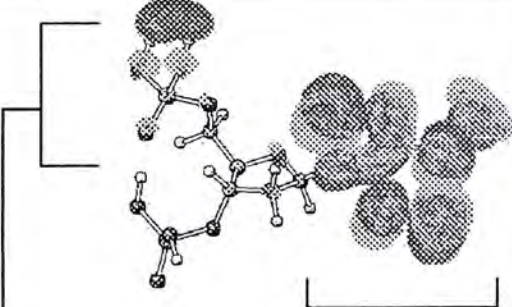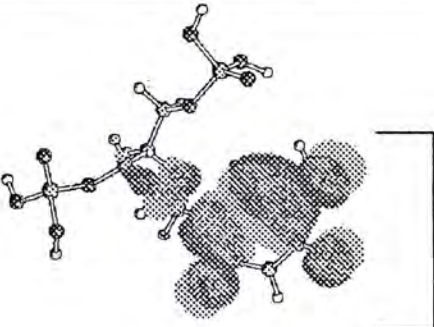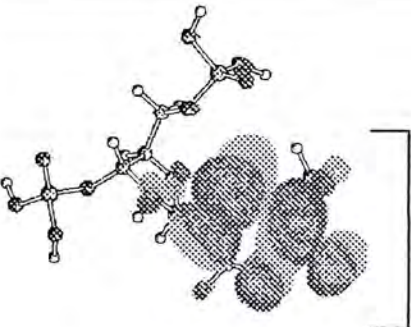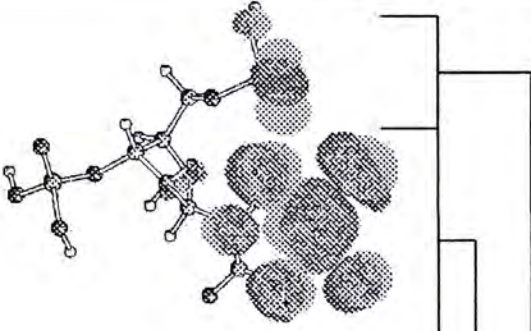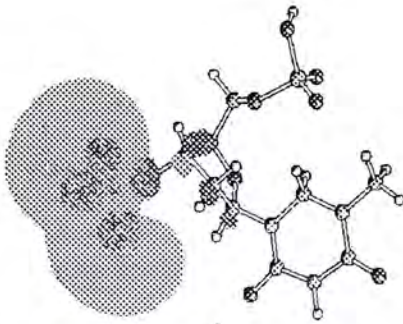
	HOMO	LUMO
G (neu)	Base	Base
G (an)	Phosphate group (P3') Base	Phosphate group (P3') Base
C (neu)	Base	Base
C (an)	Phosphate groups Base	Phosphate group (P3') Base

Table 3.31

The molecular orbital of HOMO and LUMO of adenine and thymine
at the neutral and the anionic state

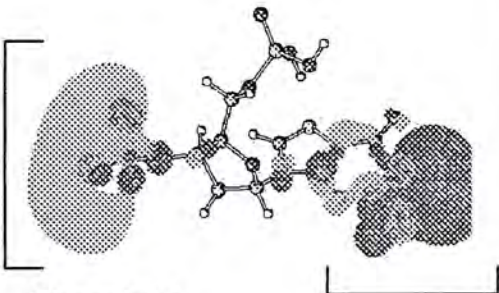|	HOMO	LUMO
Ade (neu)	Base	Base
Ade (an)	Phosphate group (P5') Base	Phosphate group (P5') Base
Thy (neu)	Base	Base
Thy (an)	Base Phosphate group (P5')	Phosphate group (P3')

nucleotides is that the sugar is not involved in the charge localization process.

In guanine and cytosine, results of charge distribution and molecular orbital show consistency. Both sets of data show that excess charges are localize evenly between the base and one of the phosphate groups. In adenine, excess charge localizes mainly in the P3' phosphate group whereas the additional charge is localized in the base of the thymine nucleotide. All results of charge distribution are consistent with the results obtained from HOMOs.

In guanine and adenine, the bond length results reveal little changes when compared against the neutral molecule, but significant changes were found for cytosine and thymine. One unique result obtained in this study is the observation of an intra-molecular proton transfer reaction occurring in thymine.

To summarize, the structure of guanine is found to be stable but its flexibility is limited. It implies that the reactivity of guanine is comparatively lower among all four nucleotides. Its structure cannot readily adapt to changes in the environment and thus recovery from damage is low. This is the reason why the damage in guanine is observed in the DNA strand. Studies reported by other workers shows that guanine is the most easily oxidized and damaged (7-15) when compared against other nucleotides. In adenine and thymine, their structures can be stabilized through compensation by the phosphate backbone, the base or by proton transfer. In comparison with guanine, their structures are more flexible and easily adapt to changes to external events.

Chapter 4
Conclusion and Future Work

4.1. Conclusion

This project focuses on a study of the changes in the structure and electronic structure of DNA nucleotides (guanine, cytosine, adenine, and thymine) at its cationic and anionic states. At the neutral state, bond lengths and torsion angles results show that the current methodology chosen is suitable because good agreement is found between the calculated results and with the experimental data. The charge distribution and molecular orbital data provide information on the properties of nucleotides when compared with the results at their cationic or anionic state.

Table 4.1 summarizes the results obtain in this thesis. In the cationic state, charges without exception depart from the DNA base, which is supported by the results of charge distribution and molecular orbitals. Due to the charge rearrangement in the base, the bond-lengths within the bases readjust to accommodate the electronic charges.

In the anionic state, the excess charge is uniquely localized on the phosphate backbone for A and T but shares almost evenly between the base and the backbone for G and C. The summary in Table 4.1 also reveals that the sugar remains relatively inert towards the events occurring on the base or on the phosphates. This poses an important question for G and C in the anionic state, which shows that additional charges are shared evenly between the base and the backbone phosphates. Since there is no change in puckering modes for the sugar in G and C in the anionic state when

compared with their neutral molecules, what would be the mechanism for the charge to be transferred to phosphates? Why has this effect not seen in A:T?

4.2. Future Work

Because all studied models are nucleotides, the effect originating from the corresponding base in basepair and the stacking effect from the neighboring base are neglected. The results obtained for the change in the torsion angles in this project cannot efficiently explain the effect and the property of DNA backbone because the latter DNA involves compromised between the preferred stacking interaction and the preferred backbone conformation. (42) There are two important mechanisms by which backbone exerts control over the base stacking geometries: (1) the backbone has finite length, and so it restricts the conformation space accessible to the bases; (2) the backbone couples the conformation properties of neighboring base steps in a sequence. Therefore, any further work conducted needs to include two nucleotides in the stand in the form of basepairs together with the backbone (phosphate groups and sugar ring as models).

Water is both importa nt to human life (59) and is an excellent solvent due to its polarity, high dielectric constant and small size, particularly for polar and ionic compounds and salts. Water ionizes and allows easy proton exchange between molecules, so contributing to the richness of the interactions in biology. Therefore, hydration is very important in the conformation chemistry and functions of nucleic acids (59 – 61, 64). B-DNA requires about 30% water to maintain its native conformation in the crystalline state; partial dehydration with lead to denaturation (59,

69

60). The anionic phosphate oxygen atoms are the most hydrated, the sugar-ring oxygen atom O(4') is intermediate, and the esterified O(3') and O(5') backbone atoms are the least hydrated. The terminal O(3') and O(5') atoms have a high affinity for solvent molecules and often participate in water bridges between symmetrically related molecules in the three helical forms. The sugar-ring oxygen atom O(4') also participate in the hydration network. It is well established that water bridges are also formed between a phosphate anionic oxygen atom and a base atom (62 – 64). However, the importance of water within the perspective of functioning as charge/proton transfer bridges are not well understood, therefore any future study should also take initiate in this direction, which may provide an understanding into the results insights into observed for G and C and thus insight into DNA damage on G.

Table 4.1

Summary of four nucleotides' results (guanine, cytosine, adenine, thymine) in this study

	Cationic			Anionic		
	Base	Sugar	Phosphate Backbone	Base	Sugar	Phosphate Backbone
Guanine						
Change in bond length	√	x	x	x	x	x
Torsion angle of backbone (out of the range)	--	--	x	--	--	x
Change in puckering Mode	--	x	--	--	x	--
Change in charge density	86 % (lose)	4 %	10 %	47 % (gain)	4 %	45 % (gain)
HOMO	√	x	√ (P5')	√	x	√ (P3')
LUMO	√	x	x	√	x	√ (P3')
Cytosine						
Change in bond length	√	x	x	√	x	x
Torsion angle of backbone (out of the range)	--	--	√	--	--	x
Change in puckering Mode	--	x	--	--	x	--
Change in charge density	85 % (lose)	7 %	8 %	50 % (gain)	6 %	44 % (gain)
HOMO	x	x	√ (3')	√	x	√ (P5')
LUMO	√	x	x	√	x	√ (P5')

Table 4.1 (Con't)

	Cationic			Anionic		
	Base	Sugar	Phosphate Backbone	Base	Sugar	Phosphate Backbone
Adenine						
Change in bond length	√	x	x	x	x	x
Torsion angle of backbone (out of the range)	--	--	√	--	--	x
Change in puckering Mode	--	√	--	--	√	--
Change in charge density	87 % (lose)	8 %	5 %	12 %	3 %	85 % (gain)
HOMO	x	x	√ (P3')	√	x	√ (P5')
LUMO	√	x	x	√	x	√ (P5')
Thymine						
Change in bond length	√	x	x	√	x	√
Torsion angle of backbone (out of the range)	--	--	x	--	--	x
Change in puckering Mode	--	√	--	--	√	--
Change in charge density	84 % (lose)	10 %	6 %	0 %	3 %	97 % (gain)
HOMO	x	x	√ (P3')	√	x	√ (P5')
LUMO	√	x	x	x	x	√ (P3')

72

Reference

1. Saenger W.; Principles of Nucleic Acid Structure, Springer-Verlag, **1984**

2. Luber Stryer; Biochemistry

3. Bloomfield V. A., Crothers D. M., Tinoco JR. I.; Nucleic Acids Structures, Properties, and Functions, University Science Books Saualito, California, **2000**

4. Blackburn G.M., Gait M.J.; Nucleic Acids in Chemistry and Biology, 2nd Ed. **1996**

5. K. B. Beckman, B. N. Ames; The American Society for Biochemistry and Molecular Biology Inc., **1997**, *272(22)*, 19633-19636

6. E. Meggers, A. Dussy, T. Shaefer, B. Giese; Chem Eur. J, **2000**, *6(3)*, 485-492

7. K. Natatani, C. Dohno, I. Satio; J. Am Chem. Soc., **2000**, *122*, 5893-5894

8. C. Dekker, M. A. Ratner; Nature, **2001**, 29-33

9. B. Giese, A. Biland; Chem. Cimmun., **2002**, 667-672

10. F. D. Lewis, X. Liu, J. Liu, R. T. Hayes, M. R. Wasielewski; J. Am. Chem. Soc., **2000**, *122*, 12037-12038

11. Scott A. P, Radom L., J .Phys. Chem., **1996**, *100*, 16502 -16513.

12. I. Satio, T. Nakmura, K. Nakatani, Y. Toshioka, K. Yamaguchi, H. Sugiyama; J. Am Chem. Soc., **1998**, *120*, 12686-12687

13. A. A. Voityuk, J. Jortner, M. Bixon, N. Roesch; Chemical Physics Letters, **2000**, *324*, 430-434

14. H. Zhang, P. Han, X. Y. Yu, X. Yan; Journal of Chemical Physics, **2002**, *117(9)*, 4587-4584

15. I. V. Kurniko, G. S. M. Tong, M. Madrid, D. N. Beratan, J. Phys. Chem. B, **2002**, *106*, 7-10

16. Y. Yoshioka, Y. Kitagwa, Y. Takano, K. Yamaguchi, T. Nakamura, I. Satio, J.

Am. Chem.Soc., **1999**, *121*, 8712-8719

17. B. Giese, Acc. Chem. Res. **2000**, *33*, 631-636

18. B. Giese, S. Wessely, M. Sportmann, U. Lindemann, E. Meggers, M. E. Michel-Beyerle; Angew. Chem. Int. Ed., **1999**, *38(7)*, 996-998

19. D. Ly, L. Sanii, G. B. Sguster; J. Am. Chem. Soc., **1999**, *121*, 9400-9410

20. M. Bixon, J. Jortner; J. Phys. Chem. B. **2000**, *104*, 3906-3913

21. F. C. Grozeman, Y. A. Berlin, L. D. A. Suebbeles; J. Am. Chem. Soc., **2000**, *122*, 10903-10909

22. R. E. Holmlin, P. J. Dandliker, J. K. Barton; Angew. Chem. Int. Ed. Engl., **1997**, *36*, 2714-2730

23. D. M. A. Smith, L. Andamowiez; J. Phys. Chem. B; **2001**, 105, 9345-9354

24. F. D. Lewis, Y. Wu; Journal of Photochemistry and Photobiology C: Photochemistry Reviews, **2001**, *2*, 1-16

25. J. Olofsson, S. Larsson; J. Phys. Chem. B., **2001**, *105*, 10398-10406

26. E. Meggers, D. Kusch, M. Spichty, U. Wille, B. Giese; Angew. Chem. Int. Ed., **1998**, *37(4)*, 460-462

27. V. Sartort, E. Boone, G. B. Schuster; J. Phys. Chem. B, **2001**, *105*, 11057-11059

28. P. T. Henderson, D. Jones, G. Hamikian, Y. Kan, G. B. Schuster; PNAS, **1999**, 96, 8353-8358

29. S. Steenken; Biol Chem., **1997**, *387*, 1293-1297

30. M. Bixon, J. Jornter; J. Am. Chem. Soc., **2001**, *123*, 12556-12567

31. G. B. Schuster; Acc. Chem. Res., **2000**, *33*, 253-260

32. B. Giese, M. Spichty, S. Wessely; Pure Appl. Chem., **2001**, *73(3)*, 449-453

33. S. S. Wesolowski, M. L. Leininger, P. N. Pentchev, H. F. Schafer III; J. Am. Chem. Soc., **2001**, *123*, 4023-4028

34. A. O. Colson, B. Besler, M. D. Sevilla; J. Phys. Chem. **1992**, *96*, 9787-9794

35. A. O. Colson, B. Besler, D. M. Close, M. D. Sevilla; J. Phys. Chem. **1992**, *96*, 661-668

36. A. O. Colson, B. Besler, M. D. Sevilla; J. Phys. Chem. **1993**, *97*, 8092-8097

37. Colson A. O., Sevilla M.D.; J. Physical Chem. , **1995**, *99*, 3867-3874

38. Colson A. O., Besler B., Sevilla M.D.; J. Physical Chem. , **1993**, *97*, 13852-13859

39. Colson A. O., Besler B., Sevilla M.D.; J. Physical Chem. , **1995**, *99*, 1060-1063

40. Richardson N. A, Wesolowski S. S., Schaefer III H. F.; J. Phys. Chem. B, **2003**, 107, 848-853

41. Sevilla M. D., Besler B., Colson A. O., J. Phys. Chem., **1995**, *99*, 1060-1063

42. Li Z., Cai Z., Sevilla M. D.; J. Phys. Chem. B., **2001**, *105*, 10115-10123

43. Richardson N. A, Wesolowski S. S., Schaefer III H. F.; J. Am. Chem. Soc., **2002**, *124*, 10163-10170

44. Richardson N. A, Wesolowski S. S., Schaefer III H. F.; J. Phys. Chem. B, **2003**, *107*, 848-853

45. Frisch A., Frisch M. J.; Gussian 98 User's Reference, Gussian, Inc., **1998**

46. Hehre W.J., Radom L., Schleyer P. v.R., Pople J. A.; Ab Initio Molecular Orbital Theory, A Wiley-Intersience Publication, **1986**

47. Weihold F.; Natural Bond Orbital Analysis Programs, NBO 5.0 Program Manual, Boardof Regents of the University of Wisconsin System, **1996-2000**

48. Greenwood N. N.; Principles of Atomic Orbitals, Royal Institute of Chemistry, Revised Edition, **1969**

49. Rauk A.; Orbital Interaction Theory of Organic Chemistry, Wiley Interscience, 2nd Ed, **2001**

50. Takashima H., Kitamura K., Tanabe K., Nagashima U.; Journal of Computational Chemistry, **1999**, *20(4)*, 443-454

51. Kryachko E. S., International Journal of Quantum Chemistry, **2002**, *90*, 910-923

52. Sponer J., Leszczynski J., Hobza P.; Journal of Biomolecular Structure & Dynamics, **1996**, *14(1)*, 117-134

53. Kabelac M., Kratochvil M., Sponer J., Hobza P.; Journal of Biomolecular Structure & Dynamics, **2000**, *17(6)*, 10711-1086

54. Neidle S.; Oxford Handbook of Nucleic Acid Structure, Oxford University Press, 1999

55. Foloppe N., Hartmann B., Nilsson L., Mackerell A. D. Jr.; Biophysical Journal, **2002**, *82*, 1552-1569

56. Packer M. J., Hunter C. A.; J. Mol. Biol., **1998**, *280*, 401-420

57. Pechenaya V. I.; Biopolymers, **1993**, *33*, 37-44

58. Gutmann V.; The Donor-Acceptor Approach to Molecular Interactions, Plenum Press, New York, **1978**